NASA Technical Memorandum 78481

Monte Carlo Solution of Boltzmann Equation for a Simple Model of Highly Nonequilibrium Diatomic Gases — Translational Rotational Energy Relaxation

Kenneth K. Yoshikawa

April 1978

National Aeronautics and Space Administration

NASA Technical Memorandum 78481

Monte Carlo Solution of Boltzmann Equation for a Simple Model of Highly Nonequilibrium Diatomic Gases — Translational Rotational Energy Relaxation

Kenneth K. Yoshikawa, Ames Research Center, Moffett Field, California
and
Institute of Space and Aeronautical Science, University of Tokyo, Tokyo, Japan

National Aeronautics and Space Administration

Ames Research Center
Moffett Field, California 94035

NOTATION

A	parameter appearing in equation (B3)
b	impact parameter
B	parameter associated with detailed balancing (eqs. (B5) and (B6))
c	molecular speed
c_o	most probable molecule speed, $\sqrt{\frac{2kT_e}{m}}$
c_*	most probable molecule speed at the initial temperature T_1.
C	exponent in selection rule (eq. (7))
d	strength associated with intermolecular potential
E	kinetic energy
E_r	rotational energy, $k\theta_r j(j + 1)$
f	distribution function
g	relative speed
I	moment of inertia
j	rotational energy level
j_o	average energy level where $\theta_r j_o(j_o + 1) = T_e$
k	Boltzmann constant
m	magnetic quantum number; also molecular weight
M_r	momentum, $\sqrt{2IE_r}$
N	number of simulated molecules within the cell
n	number density
P	rotational transition probability
$\tilde{P}$	modified rotational transition probability
Q	collision cross section
R	intermolecular distance

t time

T temperature

u x component of velocity

v y component of velocity

V interaction potential, or velocity

w z component of velocity

δ index of power associated with point centers of repulsion model, (eq. (6)), $V(R) = d/R^{\delta}$.

Δ rotational level jump

Θ_r characteristic rotational temperature

Λ relaxation time, (eq. (16))

μ reduced mass

ν collision frequency

σ effective collision diameter

τ characteristic collision time based on equilibrium translational temperature, $1/(n\pi\sigma^2 c_o)$

χ deflection angle defined in equations (2) or (10).

Ω solid angle

Subscripts:

e equilibrium

i,j rotational states

max maximum value

r rotational

t translational

Superscript

$\rightarrow$	vector
$'$	after
(ℓ)	ℓ^{th} momentum

MONTE CARLO SOLUTION OF BOLTZMANN EQUATION FOR A SIMPLE MODEL OF HIGHLY NONEQUILIBRIUM DIATOMIC GASES

Translational Rotational Energy Relaxation

Kenneth K. Yoshikawa*

Ames Research Center, NASA
Moffett Field, California, 94035

and

Institute of Space and Aeronautical Science
University of Tokyo, Tokyo, Japan (153)

SUMMARY

Theoretical studies of translational and rotational energy relaxation in diatomic gases are described. The direct simulation Monte Carlo method is employed to solve the Boltzmann equation for a rotationally excited highly nonequilibrium gas. The gas investigated is homonuclear diatomic nitrogen, and the semiclassical model of Itikawa is incorporated for the transition probability that describes rotation-translation energy interchange.

The details of energy interchange between the translational motion and the rotational energy levels of the gas are examined for spatially uniform flow without boundary interactions (the "box" calculation) with a variety of initial conditions. The results show:

1. The assumption that relaxation occurs via successive local Maxwellian velocity distributions, which is a commonly used basis for finding approximate solutions of Boltzmann equation, is not valid for gases that are initially in highly nonequilibrium states. This is especially true for initial conditions that involve low translational and high rotational temperatures.

2. The energy distributions for such transitions show bimodal (or double peak) relaxation patterns; the secondary peak ("satellite peak") appears around the Maxwellian elastic peak in the velocity distribution early during the relaxation period. The secondary peak is due to inelastic collisions and is analogous to the rotational Raman effect accompanying Rayleigh scattering.

3. The rotational energy distribution also shows bimodal relaxation effects: In addition to thermal equilibrium Boltzmann peak, a weak peak also appears at the high rotational energy levels. When the rotational energy

---

*Visiting staff. On leave from Ames Research Center during 1976-1977.

distribution is a delta function, however, relaxation proceeds only as a single-peak distribution. One, therefore, concludes that single- or double-peak relaxation depends on the type of initial distributions assumed.

4. Relaxation of the velocity distribution to equilibrium Maxwellian occurs relatively fast while the rotational energy relaxes more slowly. The relaxation time depends not only on equilibrium temperature, but also on initial velocity and rotational energy distributions.

Close correlation of the relaxation between the box models and fluid flows, such as, sound absorption, shock wave, and free-jet expansion experiment are described. Also presented are brief preliminary results of a shock wave showing translational and rotational energy relaxation structure.

A 16-mm movie film displays examples of the relaxation effects of the "box" model with a variety of initially specified velocity and rotational energy distributions.

INTRODUCTION

A knowledge of internal energy transfer mechanisms at the molecular level is valuable for an accurate understanding of many important nonequilibrium problems that occur in high-speed gas dynamics, acoustics, laser transmission, detonation, combustion, pollution, and atmospheric physics. For example, collision-induced rotational transitions play a major role in establishing the population inversions leading to gas-dynamic laser action, and also in evaluating the effects of highly nonequilibrium energy transfer in rarefied gas flow about spacecraft entering the planetary atmosphere.

In the present paper, several new and important results are presented on internally excited translation-rotation energy relaxation. These results are obtained by solving the Boltzmann equation by the Monte Carlo direct simulation method, which previously has been applied successfully to monatomic (without internal rotational relaxation) gas flow problems (refs. 1 to 3). An important feature of the simulation method is that it provides insight into the effects of collisional relaxation at the microscopic level. In particular, the instantaneous internal energy distributions can be continuously observed throughout the relaxation processes. To ensure that these distributions be meaningful, however, it is essential that the rotational transition probability function, used in the method, display certain features; namely, (1) probability must be conserved, (2) probabilities relating transitions to and from pairs of definite states must satisfy "detailed balancing," and (3) probabilities, when used in the simulations, must yield the correct asymptotic behavior of the distributions (refs. 4 and 5).

The Monte Carlo method itself can be described briefly as follows (see refs. 2 and 3 for details): The flow is determined by following a statistical sample comprising several thousand molecules that are allowed to collide with each other. The phase space coordinates that involve trajectory and rotational

variables are known at every instant. These coordinates are allowed to change only during a collision; the modeling of these intermolecular encounters is, of course, the essential part of an accurate simulation. To account for these sampling encounters, a molecule and a near neighbor are each selected at random as are also their impact parameter and relative orientation angles — all in a manner representative of typical molecules undergoing similar encounters. They are accepted for a collision or rejected according to a selection rule that is dependent on the collision cross section. Since the initial coordinates, that is, relative velocity, impact parameter, orientation angles, and pair of rotational quantum states, are known, the final rotational quantum states can be computed. This involves computing the transition probabilities of all quantum states that are accessible from the known initial states and then selecting randomly from this resulting distribution.

The procedure used here for the "translational" interactions parallels other investigations (refs. 1 and 3) which treat of monatomic gases only. The procedure is different, however, from those investigations that have treated of translation-rotation interactions. All investigations are easily categorized under the following descriptions: (1) semiempirical, (2) classical, (3) semiclassical, and (4) quantum mechanical. Within these categories, the semiempirical treatment includes an energy sink (ref. 6) and rough spheres and loaded spheres (ref. 7) to model the translation-rotation collision processes. While such methods do not appear to be satisfactory for highly nonequilibrium flow, they adequately describe near equilibrium steady flows. The classical models (refs. 8 and 9), although consistent with the classical direct simulation Monte Carlo procedure used here, necessarily include approximations to make the models tractable for studies of the type considered in this report. The approximations yield appropriate macroscopic behavior for a nonequilibrium example, but do not adequately provide limiting microscopic behavior. In particular, individual molecular encounters that violate energy and momentum conservation can occur.

Semiclassical methods (refs. 4, 5, and 10) appear to have physically realistic bases. The simplified model of Pearson and Hansen satisfies limiting equilibrium behavior, but, during a calculation, the model causes a drift in the answers that violates energy equipartition (ref. 4). Itikawa's model is more rigorously founded, allows for treatment of molecular collisions (ref. 5), and also satisfies conservation of probability and appropriate detailed balancing. Itikawa's model, therefore, satisfies the desirable characteristics of the ideal model that we described earlier; our investigations described in this paper depend on this model. Our intent, then, is to extend its application to even more general problems.

As regards the fourth category of the model (i.e., quantum mechanical models), the author is not aware that truly quantum mechanical results are yet viable. Such descriptions are difficult to obtain analytically, and to apply.

In this paper, we treat translation-rotation interactions for a spatially uniform gas far removed from solid boundaries. We are concerned only with a basic understanding of translation-rotation relaxation behavior in highly

nonequilibrium situations. In fact, it is our belief that the Monte Carlo method is best suited for studies of the type described in this paper.

The results presented are based on calculations involving three different basic types of initial conditions: (1) equilibrium, (2) nonequilibrium-equipartition (i.e., equipartition is satisfied, but distributions are perturbed), and (3) nonequilibrium-nonequipartition (i.e., both the equipartition and the distributions are perturbed). Also included are the results of monatomic gas simulations (rotational relaxation effects frozen) to assist comparisons with coupled translation-rotation relaxation simulations. To further assist the understanding of the Monte Carlo method, the essential mathematical relations are also given in this report.

FORMULATION AND PROCEDURE

The essence of the Monte Carlo procedure is described briefly in the Introduction. Introduced in this section are several analytical relations that assist both the understanding and use of the method. Appendices A and B provide supplementary analysis to the procedure and appendix C is a listing of the computer program that was used in the procedure.

Governing Equations

The study described in this paper concerns the temporal and spatial relaxation of the velocity and rotational energy state distributions that characterize a statistical sample representing several thousand molecules. If we assume that the molecular distributions themselves are diagonal and independent of the degenerate rotational m substates, the Boltzmann equation (or Wang, Chang and Uhlenbeck equation, see ref. 11) that relates the temporal and spatial behavior of the distribution functions f_i can be written

$$\frac{\partial(nf_i)}{\partial t} + \vec{V}_i \cdot \vec{\nabla} f_i = \sum_{ji'j'} \iint n^2 \left[\frac{(2i+1)(2j+1)}{(2i'+1)(2j'+1)} f_{i'} f_{j'} - f_i f_j \right] g \frac{d\sigma}{d\Omega} d\vec{\Omega}\, d^3V_2 \quad (1)$$

where n is the number density, $f_i = f_i(\vec{x}, \vec{V}, t)$ is the distribution function which depends on time t, position $\vec{x}$, velocity $\vec{V}$, and rotational state i, $d\sigma/d\Omega$ is the differential cross section corresponding to solid angle Ω. External forces are assumed to be absent. The Monte Carlo procedure is used to effectively solve this equation by means of a probabilistic sampling procedure. Implicit within the equation and procedure are the conventional fluid dynamic conservation laws (i.e., conservation of mass, momentum, and energy; see, e.g., ref. 11).

Of greatest interest for the study given here is the "box" calculation wherein the gas is spatially uniform, has constant density, and is stationary; that is, the gas is entirely contained within an "imaginary box" that has unit

volume and noninteracting boundaries (sketch (a)). The procedure, in this case, concerns interactions in a closed system. Energy conservation is applied directly (i.e., exact energy conservation is imposed on the interacting pairs of molecules) and "random sampling" ensures that, over long periods of time, the number of molecules contained within the box remain constant. These concepts are treated in greater detail in the subsequent discussion.

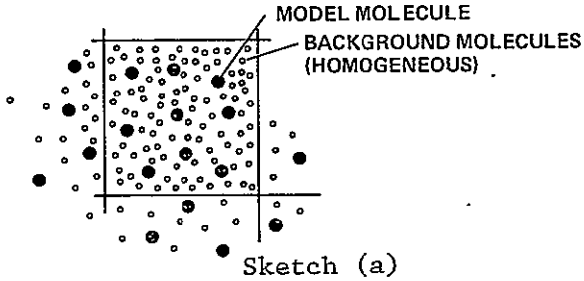

Sketch (a)

The "box" calculation has general utility since such a calculation, when started with an appropriate set of initial conditions, provides insight into mechanisms in the more general flow situation as found in sound absorption, normal shock wave, or free jet expansion experiments (see table I). In addition to the "box" calculation results, a simulation is also given for steady one-dimensional shock wave flow. This result is preliminary and demonstrates the capability of the method for simulating more complicated flows.

Collision Parameters

The essence of an accurate simulation is the random or probabilistic sampling used to select the interacting (colliding) molecular pairs, to determine whether a reaction occurs, to find the resulting "states," and then to advance the time interval for the next collision, and so on. To provide insight on this entire collision process and to arrive at a criterion for evaluating certain of the parameters required to define a collision, it is worthwhile to briefly review the classical representation of the equivalent process, and to observe how such relations depend on intermolecular potential.

A classical representation (ref. 7, ch. 8) is given by

$$\chi(b,g) = \pi - 2 \int_{R_C}^{\infty} (b\ dR/R^2) \Big/ \sqrt{1 - (b/R)^2 - V(R)/(1/2)\mu g^2} \qquad (2)$$

$$Q^{(\ell)}(g) = 2\pi \int_{0}^{\infty} (1 - \cos^{\ell} \chi) b\ db \qquad (3)$$

where $V(R)$ is a spherically symmetric intermolecular potential, $\chi(b,g)$ is the encounter deflection angle, which depends on impact parameter b and on g, relative velocity of approach, μ is the reduced mass, R_C is the distance of closest approach, and $Q^{(\ell)}(g)$ is the ℓth "momentum" transport cross section, which also depends on relative velocity (for studies reported here, $\ell = 1$). The collision frequency, ν, is then given by

$$\nu = nQ^{(\ell)}g \tag{4}$$

With this relation, the collision time, Δt, between encounters and the elapsed time, t, are given, respectively, by

$$\left.\begin{aligned} \Delta t &= \frac{2}{N}\frac{1}{\nu} \\ t &= \sum_i \Delta t_i \end{aligned}\right\} \tag{5}$$

where N is the number of particles in the "box."

Collision.—For cases in which the intermolecular potential is inversely proportional to the power, δ, of distance between colliding molecular pairs, we can readily calculate a frequency ratio (e.g., ref. 5)

$$\left(\frac{\nu}{\nu_{max}}\right) = \left(\frac{g}{g_{max}}\right)^{(\delta-4)/\delta} \tag{6}$$

where ν_{max} and g_{max} are the maximum possible values in a cell. The dimensionless ratios of frequency and relative approach velocity are related through δ. If the collision process can be represented by symmetric inverse power-law potentials, then equation (6) is a valid representation for all collisions and can be used as a criterion to decide whether an "encounter" is a "collision." The representation, therefore, serves as a "selection rule" for encounters.[1]

For the Monte Carlo results displayed in this report, we have arbitrarily picked intermolecular potentials with $\delta = 4$ (i.e., "Maxwell molecules").

Of all encounters that are collisions, we must further categorize those which are elastic from those which are inelastic (i.e., those which yield rotational transitions).

Inelastic collision.—Not all collisions result in a rotational transition. For example, some interacting pairs may have insufficient relative energy to

[1]Actual intermolecular potentials have a more complex behavior than the idealized δ potential upon which equation (6) is based. Relations equivalent to equation (6), but based on more accurate representations for the molecular potential, can be found in reference 12. The expressions were derived recently and, hence, were not available for the simulations described in this paper.

induce a transition. To separate such events from those which result in rotational transitions (i.e., inelastic collisions), we introduce a relation similar to that given above but with a different value for the exponent, that is,

$$\left(\frac{\nu}{\nu_{max}}\right)_i = \left(\frac{g}{g_{max}}\right)^{C_i} \tag{7}$$

where the subscript i denotes inelastic collision. The appropriate value to use for C_i, however, is based on simulation results. We require that simulations, which start with Maxwell-Boltzmann distributions that satisfy equipartition, must yield nondrifting results. A value of $C_i = 0.431$ yields this desired behavior. The procedure used to evaluate C_i is also described in reference 5, but in greater detail.

Collision Dynamics

In the previous section, the parameters required to determine the occurrence of a collision are given. In this section, we describe the procedure for finding the trajectories after a collision. A collision, of course, also can be accompanied by rotational transitions in either or both colliding pairs of molecules. These rotational transitions can also perturb the particle trajectories. In this section, we describe the relations that ensure collision symmetry (i.e., a collision is invariant with its inverse) and that enable rotational transitions to be more precisely determined.

The relative velocity and impact parameter after a collision are obtained by knowing the onset energy and momentum. The relations are given by

$$(g')^2 = g^2 - \frac{2}{\mu}\left(E'_{r1} - E_{r1} + E'_{r2} - E_{r2}\right) \tag{8}$$

and

$$b' = \frac{\left[gb - \left(M'_{r1} - M_{r1} + M'_{r2} - M_{r2}\right)/\mu\right]}{g'} \tag{9}$$

where E_r and M_r are the rotational energy and momentum before a collision and a prime distinguishes the corresponding values after a collision. We assume that rotational transitions only slightly perturb the relative velocity and impact parameter.

The deflection angle, given by equation (2), is actually dependent on the functional behavior of the intermolecular potential, but, for finding the limiting trajectories, we assume that the infinite-rise potential (i.e., a "billiard ball" collision) is adequate. The corresponding deflection angle is given by

$$\chi(b) = 2 \cos^{-1}\left(\frac{b}{\sigma}\right) \tag{10}$$

where σ is the effective diameter of the rigid-spherical molecule. The slightly perturbing effect of inelastic collisions resulting from the rotational transitions is accounted for by the following average:

$$\bar{\chi}(b) = \frac{\chi(b) + \chi(b')}{2} \tag{11}$$

To completely specify a collision, however, it is also necessary to give the orientation angle ε, which references the collision plane with respect to some arbitrary coordinate plane (see, e.g., ref. 13, p. 36). The velocity components before and after the collision can be related (e.g., ref. 13)

$$g_x' = \frac{g'}{g}\left(g_x \cos\bar{\chi} - \sqrt{g^2 - g_x^2}\cos\varepsilon \sin\bar{\chi}\right) \tag{12a}$$

$$g_y' = \frac{g'}{g}\left[g_y \cos\bar{\chi} + (g_x g_y \cos\varepsilon + g\, g_z \sin\varepsilon)\sin\bar{\chi}/\sqrt{g^2 - g_x^2}\right] \tag{12b}$$

$$g_z' = \frac{g'}{g}\left[g_z \cos\bar{\chi} + (g_x g_z \cos\varepsilon - g\, g_y \sin\varepsilon)\sin\bar{\chi}/\sqrt{g^2 - g_x^2}\right] \tag{12c}$$

We impose conservation of linear momentum to find the resulting velocity components after a collision. There results

$$\left.\begin{aligned} u_2' &= \frac{1}{2}(u_1 + u_2 + g_x') \\ v_2' &= \frac{1}{2}(v_1 + v_2 + g_y') \\ w_2' &= \frac{1}{2}(w_1 + w_2 + g_z') \end{aligned}\right\} \tag{13a}$$

$$\left.\begin{aligned} u_1' &= u_2' - g_x' \\ v_1' &= v_2' - g_y' \\ w_1' &= w_2' - g_z' \end{aligned}\right\} \tag{13b}$$

Rotational Transition Probability

To describe inelastic collisions, also needed, in addition to the trajectory parameters introduced in the previous sections, are expressions which relate the probability of transition between initial and final rotational energy states (i.e., the rotational transition probabilities). As was pointed out in the introduction, the semiclassical probabilities derived by Itikawa (ref. 5) are used. A brief description of their properties follows.

We describe an interaction where rotational transitions occur from levels (i,j) to (i',j') by

$$N_2(i) + N_2(j) \rightarrow N_2(i') + N_2(j') \tag{14}$$

The collision trajectory itself, as described earlier, is determined classically: Given an analytical relation for the trajectory, the amplitude of the rotational transitions can then be determined from quantum mechanical considerations. By appropriately combining the trajectory with an expanded set of Schroedinger equations (e.g., see ref. 5), the amplitude of the rotational transitions can be obtained by solving a set of coupled differential equations. In order to reduce the rank of the system, the effective potential method of Rabitz (ref. 14) is employed. The method eliminates the dependence of the interaction matrix on the magnetic quantum number, m. The resulting coupled set of ordinary differential equations are then solved by using the exponential approximation (see ref. 15). What is important is that the method treats an interaction regardless of its "strength," and, in addition, allows for the likelihood of all transitions, including those with multilevel jumps. The simultaneous transitions for both colliding molecules (i.e., rotation-rotation as well as rotation-translation) are also taken into account. The precise formulation used is given in reference 5.

Some important properties of the probabilities that pertain to the Monte Carlo simulation method are described briefly in appendix B. If a collision is inelastic as selected by equation (7), the transition of pair's molecular states are then determined by the Itikawa's rotational transition probabilities.

RESULTS AND DISCUSSION

In this section, Monte Carlo simulations are described for a stationary homogeneous molecular gas (i.e., for a "box" calculation). The simulations differ depending on the choice of the initial distribution functions (see table 1). The initial conditions fall under three general categories: (1) complete equilibrium, (2) nonequilibrium, equipartition, and (3) nonequilibrium and nonequipartition. We use the term nonequilibrium here to denote that either the velocity distribution, f_t, or the rotational energy distribution, f_r, are non-Maxwellian.

The first case, that is, complete equilibrium, tests the method, as well as the internal parameters, for self-consistency. The velocity and rotational energy distributions should remain constant for extended periods of calculation. That is, the internal energy distributions should remain Maxwellian and equipartition should be inviolate (e.g., refs. 4 and 5).

The second case, where the velocity and rotational energy distributions are specified to satisfy energy partition (i.e., the fraction of energy distributed between translation and rotation is proper, but where the distributions, themselves, are non-Maxwellian) provides a test on whether the procedure has an internal driving mechanism that will yield a relaxation to equilibrium within a physically realistic time.

The third set of initial conditions, where the initial distributions violate both equipartition and are highly nonequilibrium states, allows even more complex investigations. For example, one can study the relaxation processes to equipartition as well as how the velocity and rotational distributions interact during the relaxation. In effect, these simulations with varied starting conditions give qualitative information on the coupling of the energy distributions and quantitative data on the rates of relaxation.

In table 1, the specific choice of initial conditions for the simulations described in this paper are listed. These results are also useful in providing qualitative information that can be used to interpret results in several equivalent experiments. The experiments are sound absorption, shock-waves, and free-jet expansions (ref. 11). Table 1 lists the simulation and the related experiment type. The simulations are described in the discussion that follows.

Initial distributions: complete equilibrium.—The first test of a good method for simulating solutions to Boltzmann's equation is that Maxwellian energy distributions, both in velocity and in rotational energy, not change for extended calculation periods. In figure 1a are given the results of such a simulation. The results show sets of paired figures for progressively increasing times corresponding to $t/\bar{\tau} = 0.0$, 1.0, 5.0, and 10.0. One figure in the pair is a snapshot of the rotational energy distribution function, f_r, plotted versus rotational energy level j at a definite time t/τ, and the other figure is the velocity distribution function, f_t, plotted versus velocity c/c_0, where c_0 is the most probable molecular speed defined by $c_0 = \sqrt{2\ kT_e/m}$, m is the molecular mass, and T_e is the equilibrium temperature associated with the "box" model. We observe that, although small fluctuations occur around the dotted curves (which represent the true Maxwellian distributions) during the calculation period, these fluctuations do not grow (ref. 5). In fact, figure 2b shows the results of the same calculation, but where the time average of the distributions, given by

$$\bar{f}_{r \text{ or } t} = \frac{1}{t} \int_0^t f_{r \text{ or } t}\, dt \qquad (15)$$

are plotted. We observe that the fluctuations are negligible in the second group of "snapshots." These simulations illustrate that, indeed, the procedure is stable over long calculation periods. The next case tests the capability of the procedure to drive arbitrarily specified initial distributions to the Maxwellian limit.

Initial distributions: non-Maxwellian velocity and rotational effects frozen.—The Monte Carlo method allows for considerable flexibility regarding the precise specification of the initial distributions. For example, one can freeze the rotational relaxation effects and investigate only the relaxation of the velocity distribution. The next example is of this type. In figure 2 are displayed the resulting time history for relaxation of the velocity distribution function, starting with two different initial distributions. In figure 2a are displayed the relaxation processes that correspond to initially letting every molecule have a speed equal to $\sqrt{3/2}\ c_0$. The dotted curve is a Maxwellian distribution characterized by the temperature $T_e = 320$ K. In this example, the "Dirac delta function" type of initial distribution should relax to coincidence with the dotted curve. The rotational energy, of course, is ignored. We observe that the distributions are largely equilibrated by the instant $t/\tau = 1$ (the area differences between the solid and dotted curves correspond to the number of molecules that still have initial velocity $\sqrt{3/2}\ c_0$ and remain to be "equilibrated"—i.e., about 10 percent of the total). At $t/\tau = 2.0$, the distribution is established and very little change occurs thereafter. One concludes from this simulation that the procedure leads to the correct Maxwellian limit, as indeed it should. In figure 2b, the initial distribution is slightly different. In this case, the energy, corresponding to kT_e, is distributed at two separate initial velocities: $c_0/2$ and $\sqrt{11}/2\ c_0$. The rotational energy is managed in the same manner as the example in figure 2a. The result for this case is nearly the same. In fact, little difference can be observed in a comparison of the relaxation history. At the instant $t/\tau = 1.0$, roughly the same fraction of molecules remain to be equilibrated as in the first example. The distribution appears to be established by the instant $t/\tau = 2.0$ and changes very little thereafter.

Initial distributions: Maxwellian velocity and equipartition.—Our next simulation, figure 3, illustrates the relaxation effects that occur when the initial velocity distribution is Maxwellian and the rotational distribution, which satisfies energy equipartition, approximates a delta function centered at $j_0 = 10$ (i.e., every molecule has kT_e rotational energy in the 10th energy level). This rotational level also represents the probable rotational energy level for a Boltzmann distributions at temperature kT_e (i.e., j_0 is found from $k\theta_r\, j_0(j_0 + 1) = kT_e$, where $\theta_r(N)_2 = 2.9$ K and $T_e = 320$ K).

Since our investigation concerns homonuclear nitrogen, only rotational transitions that satisfy the multiples of $\Delta j = \pm 2$ are allowed. At the first instant displayed in figure 3 after relaxation begins (i.e., at $t/\tau = 0.5$), we observe a double peak appearing in the velocity distribution. This behavior is very similar to the Stokes and anti-Stokes lines that appear in Raman scattering (ref. 16). The position of these peaks can be calculated (see appendix A) and appear at the velocities $c/c_0 = 0.91$ and 1.1, respectively.

These peaks appear because the rotational energy is "dumped" into a narrow energy band. The transitions, $\Delta j = \pm 2$, are most probable compared to multilevel transitions, $|\Delta j| \geq 4$. This effect results in two perturbations appearing in the velocity distribution about the most probable velocity c_0.

Initial distributions: Maxwellian velocity ($T_t > T_e$) and nonequipartition.— The simulation displayed in figure 4 demonstrates the relaxation effects caused by violating equipartition. Rotational energy states are assumed initially to be unexcited; the energy is contained entirely within the velocity distribution which is Maxwellian ($T_t = 534$ K). The fact that single level ($\Delta j = \pm 2$ for homonuclear molecules) rotational transitions are the most likely compared to multilevel ($|\Delta j| \geq 4$) transitions is also apparent here. After relaxation begins, we observe that the lowest level rotational states populate first. The gain in rotational energy appears to be at the expense of the molecules with velocities that correspond to the most probable velocity c_0 or higher. As the time t/τ increases, energy continues to be "dumped" from the translational to the rotational mode as demonstrated by the downward drifting velocity distribution and the upward drifting rotational distribution. These processes become less efficient as energy is "dumped" to higher and higher rotational energy levels. This is apparent because, as the width of the energy level increases, the energy interchange between the rotational and translational mode becomes even less efficient. We find, then, that considerable time is required to populate the uppermost rotational energy levels. In fact, the velocity distribution appears to be nearly equilibrated by the time $t/\tau = 20.0$, while the rotational distribution is still relaxing at $t/\tau = 50.0$.

The simulation demonstrates that the step-wise populating mechanism implicit within the Itikawa model leads to relatively slow relaxation to a Boltzmann rotational distribution. Of course, if multiple level transitions were more effective, the rate of relaxation to a Boltzmann rotational distribution would be greatly enhanced. These features are characteristic of translation-rotation transitions, and they are apparent in all simulations involving translation-rotation interactions.

The simulation displayed in the next figure, figure 5, differs from this example in that rather than follow the populating of the rotational energy levels from an initial state of "excessive" translational energy, we follow the depopulating of the rotational energy levels from an initial state of "excessive" rotational energy. Of course, "excessive" refers to the manner in which that energy is initially distributed relative to the distribution that satisfies equipartition.

Initial distributions: Maxwellian velocity ($T_t < T_e$) and nonequipartition.— In figure 5a, we observe that, at the initial instant prior to relaxation, the rotational energy is stored in a Boltzmann distribution ($T_r = 793$ K) which peaks near the most probable levels $j = 10$ or 12 (i.e., $f_r(x)$ is maximum at $x = 11.16$). The velocity distribution, however, peaks at low velocities, $c^*/c_0 = 0.135$.

Several interesting features can be observed during the relaxation processes. We note that a satellite peak (refs. 16 and 17) develops on the high

sides of the velocity distribution (i.e., $c/c_0 \simeq 0.44$), and this peak forms at the expense of rotational energy near the most probable levels $j = 10$ or 12 (as exemplified by the "dip" in the rotational distribution). This peak continues to grow as rotational energy is converted to thermal motion. Again, one observes the effect of the inefficient coupling of translational and rotational energy interchange with the higher rotational energy levels. This effect, of course, results in the appearance of a second peak at the higher rotational levels. This effect of double peaks is also discussed by Polanyi and Woodall (ref. 18). The peaks remain in the distribution until quite late during the relaxation process (say, $t/\tau = 50.0$). We also notice that, by this time, the velocity distribution has nearly equilibrated to Maxwellian, and this occurs before the rotational distribution becomes Boltzmann, similar to what occurred in the previous example, figure 4.

Also interesting is a comparison of how close the distributions approximate the Maxwell-Boltzmann distribution during each instant of the relaxation processes. Such comparisons are displayed in figure 5b. Here, the dotted curves are "local Maxwell-Boltzmann" distributions rather than the asymptotic limiting equilibrium distributions displayed heretofore. The dotted distributions are determined by matching the energy, in both the velocity and rotational modes, with the simulation results. These results illustrate that the actual distributions found by the simulation deviate significantly from local Maxwell-Boltzmann distributions. This demonstrates that the popular methods that rely on expansion procedures involving local Boltzmann distributions for solving the Boltzmann equation can be unreliable. In fact, the double-peaked results displayed in figure 5 illustrate that appropriate distributions can have rather complex non-Boltzmann functional behavior.

Initial distributions: Maxwellian velocity ($T_t < T_e$) and nonequipartition.— The simulation displayed in figure 6 is very similar to that displayed in figure 3; the initial rotational energy distribution approximates a Dirac delta-function, but the simulation differs in that the constant rotational energy assigned each molecule violates equipartition. Here we have an initial dumping of the rotational energy into the 16th rotational energy level. The velocity distribution, however, is Maxwellian. At the onset of relaxation, we observe the "anti-Stokes" Raman scattering effect appearing in the velocity distribution, that is, the appearance of a satellite peak (using the relations in appendix A with $j = 16$ and $\Delta j = -2$, we find the peak location to be $c/c_0 = 0.55$). The pumping mechanism by which the high rotational energy is converted into thermal motion also appears conspicuously in this example (see ref. 17). The single step transitions from the 16th to 14th level ($\Delta j = -2$) occur first with the quanta of rotational energy being preferentially absorbed by the very low-speed molecules. As this process proceeds, the number of molecules in the 14th level approaches equality with the number in the 16th level. Simultaneously, the "anti-Stokes Raman" peak broadens as the slow speed molecules are "pumped" into this region. As the relaxation progresses, the lower lying rotational levels are successively populated while the "anti-Stokes Raman" peak becomes increasingly broad.

Contrary to the previous example, figure 5a, the rotational distribution relaxes continuously with one one peak. The velocity distribution, however,

similar to that in figure 5, displays a slow relaxation to the Maxwellian distribution. The relatively large energy in the high rotational states, the slow relaxation experienced in these states, and the strong coupling of these levels with the slow molecules all appear to contribute to inhabiting the relaxation of the velocity distribution to Maxwellian.

To show the manner by which the local distributions compare with local Maxwell-Boltzmann distributions during the relaxation processes, the dotted curves are again introduced in figure 6b, as was done in figure 5b. Again, we observe that the distributions do not approximate Maxwell-Boltzmann distributions during each instant of the relaxation.

Relaxation of Average Rotational Energy

The results displayed in figures 1 through 6 illustrate, in particular, the manner by which an initial energy distribution relaxes to the final Maxwellian distributions. Also interesting is the manner by which the "average energy" approaches some asymptotic constant value. Such results are given in figure 7. In this figure are displayed four curves. Three curves display the average energy relaxation associated with initial distributions, which are Dirac delta-function type, and the fourth displays results with an initial distribution that is Boltzmann with high rotational temperature. The essential feature is the comparison of results between curves that have high and low initial rotational energy (e.g., cases 4 and 5). Because the coupling between translation and rotation is efficient for the lower levels, the slope of these curves is greatest. Also, interesting is case 3 which illustrates that even though the initial distribution satisfies energy equipartition, the system is not bound to satisfy equipartition during the subsequent instants as the rotational distribution asymptotically approaches a Boltzmann distribution. Additional simulations all illustrate the downward shift (as illustrated in the figure for $j = 10$) followed by the upward relaxation to "equipartition."

Figure 7 can also be used to define a useful relaxation time that characterizes the simulation results. Such a definition, of course, is not exactly clear because the relaxing curves are not exponential. One can resort to the definition given by (e.g., ref. 11)

$$\Lambda = [(E_r)_e - E_r(t)]/(dE_r/dt) \tag{16}$$

This definition, however, is impractical when the energy difference in the bracket is small. One can also define the relaxation time to be that time when the bracket expression has reduced to $1/e$ of its initial value (e.g., ref. 13). On the basis of this latter definition, it turns out that $\Lambda \simeq 32$ is satisfactory for both curves labeled $j = 0$ and $j = 16$. This value also seems to be consistent with the simulation displayed for all three initial delta functions of rotational energy distribution (i.e., $j = 0$, 10, and 16) in figures 3, 4, and 6. In these figures, we can see that the relaxation appears to be nearly ceased at the same instant between the two displays of the distribution function at $t/\tau = 20$ and 40.

The relaxation of translational energy is not shown here since, for our "box" calculation, conservation of energy E_t is directly related to the average rotational energy E_r via the relation

$$E_t/(E_t)_e = 5/3 - 2/3\ E_r/(E_r)_e \tag{17}$$

at each instant during the relaxation processes. The subscript e denotes the asymptotic limiting energies associated with equilibrium.

Shock Wave Structure

The previous examples, figures 1 through 6, rely on the "box" model, which is based on the assumption that the distributions have no spatial dependence. The Monte Carlo method, of course, has potential for much greater geneality. We can effectively introduce a spatial dependence into the distributions and study more complicated problems. To demonstrate this effect, results of simulations for a normal shock wave structure are displayed in figure 8. For this example, the number of molecule in the sample size was not increased and, therefore, the curves are not exactly smooth.

In this figure are displayed the translational and rotational temperatures (based on average energy) and density at seven distinct instants of time. As one might expect, the translational temperature develops an overshoot. As the rotational mode is excited the high translational temperature decreases and approaches an asymptotic steady value.

This example is included to demonstrate that such simulations that involve both elastic and inelastic collisions are possible. More refined shock shapes than those displayed in figure 8 will require a considerable increase in the number of molecules within the statistical sample and in computation time, thus, no attempt has been made to check the convergence of the solution.

CONCLUSIONS

The Monte Carlo simulation method described in this report, including the use of the Itikawa model for representing inelastic collision processes, is a viable scheme for studying translation-rotation interactions. The method can provide very useful qualitative and quantitative information on the relaxation processes associated with at least relatively simple topological systems (i.e., one-dimensional and quasi one-dimensional systems). On the basis of experience gained here, it is not expected that the method will be considered viable at this time for more complex topological studies (i.e., three-dimensional flow simulations), because current and foreseeable computer resources appear insufficient to allow economical processing of the increased sample size that will be required in such studies.

The method, however, is very useful in its present form to visualize fundamental gas kinetic behavior as demonstrated by the results presented in this paper. A review of the simulations given in this report shows the following results:

1. Single step ($\Delta j = \pm 2$ for homonuclear molecules) transitions are the significant mechanisms of intermodal energy transfer rather than the multistep transitions (i.e., $|\Delta j| \geq 4$ for homonuclear molecules).

2. The coupling of translation-rotation transitions is the most efficient for low lying rotationally excited molecules and is least efficient for the highly rotationally excited molecules.

3. The "relaxation time" required for molecules to reach an asymptotic steady-distribution in both the velocity and rotational states is dependent on the initial distributions.

4. Relaxation occurs via a successive set of distributions that are not Maxwell-Boltzmann (nonlocal Maxwellian).

5. Initial rotational distributions with high rotational energy and that are far removed from satisfying equipartition lead to the appearance of "satellite peak" on the velocity distribution via a mechanism that is similar to the Stokes Raman effect accompanying the Rayleigh scattering.

Subsequent studies should quantitatively compare characteristic relaxation times found by the Monte Carlo methods with similar times obtained experimentally. Of course, only qualitative comparisons are given here.

The simulations reported in this paper certainly demonstrate that the method is viable for studying translation-rotation interaction processes and that some revisions are necessary in existing analytical methods.

APPENDIX A

ESTIMATE OF SATELLITE PEAK POSITIONS IN THE VELOCITY DISTRIBUTION

Certain types of rotational energy distributions can couple strongly through the collision processes to perturb the velocity distributions. In these cases, peaks occur (on the velocity distributions) that are analogous to the Stokes and anti-Stokes rotational Raman effects which accompany Rayleigh scattering. The satellite peaks have been observed experimentally (refs. 16 and 17). In one case (example 1) energy is "dumped" into a narrow band of the rotational energy levels; a pair of "satellite peaks" then appear around the maximum in the velocity distribution during subsequent relaxation. In another case (example 2) a similar effect occurs when the velocity distribution has a peak at low velocities ("cold gas") and the rotational energy is peaked at the higher levels. Here, however, only one "satellite peak" appears in the resulting velocity distribution. The nature of these peaks is such that their position can be readily estimated without solving the Boltzmann equation.

The relative velocity, g', of a pair of molecules after a collision can be found from equation (8) and is given by

$$g' = g\sqrt{1 - \Delta E_r/(1/2\ \mu g^2)} \tag{A1}$$

where ΔE_r is the change in rotational energy during a collision, and μ is the reduced mass. We assume that only one of the pair of colliding molecules transfers rotational energy during the interaction; the rotational transitions correspond to $j \to j \pm \Delta$, that is,

$$\begin{aligned} \Delta E_r(j \to j \pm \Delta) &= E_r(j \pm \Delta) - E_r(j) \\ &= \Delta \cdot (\Delta \pm (2j + 1))k\ \theta_r \end{aligned} \tag{A2}$$

where k is Boltzmann's constant, and θ_r is the characteristic rotational temperature which corresponds to a single transition. We introduce the following notation

velocity corresponding to the initial Maxwellian peak: c^*

velocity after rotational-translational interaction: c'

reference velocity: $c_0 = \sqrt{2kT_e/m}$

and, in addition, the approximations $g \simeq 2c^*$ and $g' \simeq 2\ c'$; we then obtain

$$\frac{c'}{c_0} \simeq \frac{c^*}{c_0} \sqrt{1 - \frac{\Delta E_r}{kT_e} \Big/ \left[\frac{1/2\ \mu(2\ c^*)^2}{1/2\ m\ c_0^2}\right]}$$

$$= \sqrt{\frac{T_i}{T_e}} \sqrt{1 - \frac{\Delta}{2}\left(\Delta \pm (2j+1)\right)\frac{\theta_r}{T_i}} \qquad \text{(A3)}$$

where we have used $\mu = m/2$ and $(c^*/c_0)^2 = T_i/T_e$. We recall for homonuclear diatomic molecules, such as molecular nitrogen, that multiples of $|\Delta| = 2$ rather than single transitions $|\Delta| = 1$ are allowed. In the analogy with Raman scattering, the positive sign corresponds to "Stokes" and the negative sign to "anti-Stokes" effects. In the discussion above, example 1 displays both Stokes and anti-Stokes effects; example 2, however, shows only anti-Stokes effect.

APPENDIX B

MODIFIED ROTATIONAL TRANSITION PROBABILITY

In the Introduction, we listed several properties that the rotational transition probabilities must satisfy to ensure their proper behavior for the Monte Carlo simulation method: (1) probability must be conserved, (2) probabilities relating transitions to and from pairs of definite states must satisfy "detailed balancing," and (3) the probabilities, when used in the simulations, must yield the correct asymptotic behaviors of the distributions. The third property has been covered in the text (also, see refs. 4 and 5). The first property, that is,

$$\sum_{i',j'} P(i,j \rightarrow i',j';\ g) = 1 \tag{B1}$$

is satisfied by Itikawa's relations (refs. 5 or 11) as is also collision symmetry, given by

$$P(i,j \rightarrow i',j';\ g) = P(i',j' \rightarrow i,j;\ g') \tag{B2}$$

To ensure the satisfaction of the second property listed above, we introduce the modified transition probability, $\widetilde{P}$, given by

$$\widetilde{P}(i,j \rightarrow i',j';\ g) = A(g)\,\frac{B(i,j;\ i',j')}{(2i+1)(2j+1)}\,P(i,j \rightarrow i',j';\ g) \quad \text{for } (i,j) \neq (i',j') \tag{B3}$$

This relation also satisfies the "principle of detailed balancing" given by

$$(2i+1)(2j+1)\widetilde{P}(i,j \rightarrow i',j';\ g) = (2i'+1)(2j'+1)\widetilde{P}(i',j' \rightarrow i,j;\ g') \tag{B4}$$

where $A = A(g)$ and the symmetric function $B(i,j;\ i',\ j')$ are arbitrary relations that have functional behaviors as indicated in the parentheses. Several example relations of $B(i,j;\ i',j')$ are

$$B(i,j;\ i',j') = [(2i_< + 1)(2j_< + 1)]^a \tag{B5}$$

or

$$B(i,j;\ i',j') = [(2i+1)(2j+1)(2i'+1)(2j'+1)]^{1/2} \tag{B6}$$

The notation $i_<$ is used to designate the smaller value of either i or i', and similarly for $j_<$.

Note that equation (B3) is obtained from equation (B4), since $g \simeq g'$ implies $A(g) \simeq A(g')$. Itikawa's expression derived in reference 5 is a specific example of the more general probability relation that is displayed here (e.g., Itikawa assumes $A(g) = 1$ and $a = 1$ in equation (B5)). It can be shown that the modified transition probability given by equation (B3) also satisfies "conservation of probability" and "detailed balancing."

It is worthwhile to comment that equation (7) in the text, which is the selection rule for inelastic encounters, was based somewhat on heuristic arguments and yielded qualitatively satisfactory results. We expect, however, that more accurate representations that will be based on more convincing physical arguments, which will involve $A(g)$ above, can be obtained for this equation.

APPENDIX C

PROGRAM LISTINGS

The entire program for the "Gas in an Imaginary Box" calculation is listed in this section.

Program listings consist of sample control cards, correction cards, main program listings, and sample input-data cards. Many unused cards are still in the listings, but are marked by a comment symbol "c," "c*," etc.

```
*
*
*       SAMPLE CONTROL CARDS
*
*
YOSHX,T0500.                                    STOP9,X6363,YOSHIKAWA
ACCOUNT,STGKKY,T4606.
AUDIT,ID=YOSHIKAWA.
ATTACH,TAPE11,FILE702,ID=YOSHIKAWA,PW=STGKKY,MR=1,CY=2.
ATTACH,OLDPL,ITILIBSOURCE,ID=YOSHIKAWA,MR=1.
UPDATE,F.
FTN,I,R=3,OPT=2,PL=100000.
ATTACH,IMSL,IMSLLIB,ID=AMESLIB.
LIBRARY(IMSL)
REQUEST,TAPE9,*PF.
REQUEST,TAPE10,*PF.
LDSET,MAP=X.
LOAD,LGO.
NOGO,MAIN.
RETURN,LGO.
MAIN.
CATALOG,TAPE9,DXXX903,ID=YOSHIKAWA,PW=STGKKY,MR=1,RP=999,CY=2.
CATALOG,TAPE10,DXX103,ID=YOSHIKAWA,PW=STGKKY,MR=1,RP=999,CY=2.
AUDIT,ID=YOSHIKAWA.
EXIT.
CATALOG,TAPE9,DXXX903,ID=YOSHIKAWA,PW=STGKKY,MR=1,RP=999,CY=2.
CATALOG,TAPE10,DXX103,ID=YOSHIKAWA,PW=STGKKY,MR=1,RP=999,CY=2.
AUDIT,ID=YOSHIKAWA.
"

*
*
*
*       PROGRAM LISTING
*
*
*IDENT,CORRECT
*I INI$$.18
C       OTHER RANDOM GENERATION
        KRAN=50
        DO 50 JP=1,KRAN
        R=RANF(0)
   50 CONTINUE

*DECK MONT$$
```

```
      PROGRAM MONTEC(INPUT,OUTPUT,TAPE5=INPUT,TAPE6=OUTPUT,TAPE7,TAPE8,
     1TAPE9,TAPE10,TAPE11)
      COMMON /TIME/ TO,TS,TF,TM,DTO,DTM,TN
      COMMON /CV/ MAX,MAX6,C1,RHO1
      COMMON /CONST/ W,A,VOM,SF,CO
      COMMON /RANDOM/ R
      COMMON /ANSWER/ MOM,T(4),G,DVOL,AI,POA,ROT1
      COMMON /PART/ P(5001)
      COMMON /CV1/ABCC(40,40,9)
      DATA   ABCC/ 14400*0. /
C
C
C     MONTE CARLO PROGRAM FOR GASES IN A BOX -REVISED BY K.K. Yoshikawa
C
      JUMP=0
    1 CALL INPUT(JUMP)
      IF(JUMP.GT.0) GO TO 30
   10 CALL INITAL
      CALL MOMENT
      CALL OUTPUT(M)
   30 IF(TN.GE.TM) GO TO 100
   50 CALL JPAIRS
  100 TM = TM+DTM
  200 IF(TM.LT.TS) GO TO 30
  209 CALL MOMENT
  330 IF(TM.LT.TO) GO TO 30
      CALL OUTPUT(M)
      TO=TO+DTO
  340 IF(TM.LT.TF) GO TO 30
      ENDFILE 10
      CALL EXIT
      STOP
      END

*DECK INP$$
      SUBROUTINE INPUT(JUMP)
      COMMON /TIME/ TO,TS,TF,TM,DTO,DTM,TN
      COMMON /CV/ MAX,MAX6,C1,RHO1
      COMMON /CONST/ W,A,VOM,SF,CO
      COMMON /RANDOM/ R
      COMMON /ANSWER/ MOM,T(4),G,DVOL,AI,POA,ROT1
      COMMON /PART/ P(5001)
      DIMENSION FC(40),FW(40)
C
C     DATA INPUT FOR MONTE CARLO PROGRAM ALA BIRD
```

```
C
      DIMENSION HED(18)
      READ(5,500) HED
      READ(5,501) MAX,RHO1,CO,W,A,VOM,MOM,DTM,TS,DTO,TF,D,R
   10 MAX6=5*MAX
      AI=.25*W*D**2
  120 POA=SQRT(3.14159/A)
  200 C1=CO
      DVOL = 0.5*(W/(RHO1*A))**2
      SF = RHO1*DVOL/(MAX*W)
      WRITE(6,600) HED
      WRITE(6,601) MAX,RHO1,DTM,TS,DTO,TF,CO,W,A,VOM,SF,D
  500 FORMAT(   18A4)
  501 FORMAT(  I4/   10X5E10.4,I3/(  4E10.4))
  600 FORMAT(1H1   18A4)
  601 FORMAT(* MAX=*I15//50X*RHO1=*G15.6,*;DTM=*G15.6,*;TS=*G15.6,
     1 * DTO=*G15.6//* TF=*G15.6,* CO=*G15.6,*  W=*G15.6,*; A=*G15.6,
     2*;VOM=*G15.6,* SF=*G15.6//*  D=*G15.6)
      IF(MAX.LT.0) GO TO 300
      RETURN
  300 READ(8) MOM,T,G,DVOL,W,A,VOM,SF,CO,TO,TS,TF,TM,DTO,DTM,TN,MAX,MAX6
     1,C1,RHO1,P,AI,ROT1,POA,ABCC,R
      REWIND 8
      NTMO=(TM-DTM)/DTO+0.5
  100 READ(7)  TAUBAR,NTM,MAX,COC2,EOE,FC,FW
      WRITE(10) TAUBAR,NTM,MAX,COC2,EOE,FC,FW
      IF(NTM.LT.NTMO)  GO TO 100
      TF=TF+100.*DTM
      JUMP=1
      RETURN
      END

*DECK INI$$
      SUBROUTINE INITAL
      COMMON /TIME/ TO,TS,TF,TM,DTO,DTM,TN
      COMMON /CV/ MAX,MAX6,C1,RHO1
      COMMON /CONST/ W,A,VOM,SF,CO
      COMMON /RANDOM/ R
      COMMON /ANSWER/ MOM,T(4),G,DVOL,AI,POA,ROT1
      COMMON /PART/ P(5001)
      COMMON/INIX2/ ERO
C
C     INITIAL VALUE SUBROUTINE FOR EQUILIBRIUM BOX
C
C     OTHER RANDOM NUMBER GENERATION
```

```
C     KRAN=10 50 OR 100 ETC.
C     DO 50 JR=1,KRAN
C     R=RANF(0)
C  50 CONTINUE
      ERO=0.5*W*C1*C1
      JO=SQRT(1.+.99401E16*ERO)/2.
C     CM=0.7071068*C1     ( 1/SQRT(2))*C1
C     ISEED=411111111
      TN=0.
      P(1)=0.
      DO 100 IM=1,4
  100 T(IM)=0.
C     CALCULATION OF INITIAL VALUES
C     I=0
C 130 P(1)=P(1)+1.
C     DO 200 L=2,4
C*    CALL RANDU(IX,IY,R)
C*    IX=IY
C     IL=I+L
C*200 CALL GAURND(IX,CM,0.,P(IL))
C 200 P(IL)=CM*GGNOF(ISEED)
C     ROTATIONAL ENERGY AT UPSTREAM CONDITIONS
C     CALL X2DIST(IROT)
C     P(I+6)=IROT
C 400 P(I+5)=SQRT(P(I+2)**2+P(I+3)**2+P(I+4)**2)
C     I=I+5
C     IF(I.GT.MAX6) GO TO 500
C     GO TO 130
C     READ INITIAL VALUES FROM THE FILE 11
      READ(11) P
  500 CONTINUE
      DTO=DTO*DTM*.99999
      TS=TS*DTM*.99999
      TF=TF*DTM*.9999
      TO=TS+DTO
      TM = DTM
      RETURN
      END

*DECK JPA$$
      SUBROUTINE JPAIRS
      COMMON /TIME/ TO,TS,TF,TM,DTO,DTM,TN
      COMMON /CONST/ W,A,VOM,SF,CO
      COMMON /RANDOM/ R
      COMMON /ANSWER/ MOM,T(4),G,DVOL,AI,POA,ROT1
```

```
      COMMON /PART/ P(5001)
C
C     COLLISION PAIR SELECTION FOR THE INVERSE POWER POTENTIAL PARTICLES
C
      VR=.0
   10 VM=P(5)
      NC=P(1)
   20 DO 40  I=2,NC
      J=5*I
      IF(P(J).GT.VM) GO TO 35
      IF(P(J).GT.VR) VR=P(J)
      GO TO 40
   35 VR=VM
      VM=P(J)
   40 CONTINUE
   50 GM=VM+VR
   60 R=RANF(0)
   80 J1=P(1)*R+1
   90 R=RANF(0)
  110 J2=P(1)*R+1
  120 IF(J1.EQ.J2) GO TO 90
      J1=5*J1-3
      J2=5*J2-3
  150 G=SQRT((P(J1)-P(J2))**2+(P(J1+1)
     1-P(J2+1))**2+(P(J1+2)-P(J2+2))**2)
C     PAIR SELECTION RULE: IF F(G/GM) > R, TAKE A PAIR
C     FOR GENERAL CASE  USE CC1 THROUGH CC3
C     F(G/GM)=(G/GM)**C
      R=RANF(0)
      FGBAR=(G/GM)**0.4310
      KELST=0
C     KELST=1  FOR MONATOMIC GAS
      IF(R.LT.FGBAR) GO TO 170
CC1   CELST=0.215 FOR EXAMPLE
CC2   FGEL=(G/GM)**CELST
CC3   IF(R.GT.FGEL) GO TO 60
CC*   THIS PROGRAM IS SET UP FOR MAXWELLIAN MODEL CASE (FGEL=1.0)
      KELST=1
C     END OF PAIR SELECTION RULE
  170 CALL CRASH(P(J1),P(J1+1),P(J1+2),P(J1+4),P(J2),
     1P(J2+1),P(J2+2),P(J2+4),KGP,KELST)
      IF(KGP.GE.1) GO TO 60
      P(J1+3)=SQRT(P(J1)**2+P(J1+1)**2+P(J1+2)**2)
      P(J2+3)=SQRT(P(J2)**2+P(J2+1)**2+P(J2+2)**2)
  260 DTN=2.*DVOL/(P(1)**2*A*G*SF)
```

```
  270 TN = TN + DTN
  280 IF(TN.LT.TM) GO TO 60
  290 RETURN
      END

*DECK CRA$$
      SUBROUTINE CRASH(U1,V1,W1, I1,U2,V2,W2, I2,KGP,KELST)
      COMMON /CONST/ W,A,VOM,SF,CO
      COMMON /RANDOM/ R
      COMMON /ANSWER/ MOM,T(4),G,DVOL,AI,POA,ROT1
      COMMON/PRBOUT/PSUM(400),RRRR,J1FIN,J2FIN
      REAL I1,I2
C     DIATOMIC PARTICLE COLLISION TRAJECTORIES
C     *ELSTIC COLLISION ; GO TO 700
      IF(KELST.EQ.1) GO TO 700
      G2=G*G
      IF(I1.GT.38..OR.I2.GT.38.) GO TO 7
      ETP=0.25*W*G2
C     EXCLUSION OF NO ENERGY TRANSITION AT LOW KINETIC ENERGY
      GO TO 1
    7 KGP=1
      RETURN
    1 R=RANF(0)
      EPS=6.28318*R
      KGP=0
      ER1=4.0241E-16*I1*(I1+1)
      ER2=4.0241E-16*I2*(I2+1)
      RM1 =SQRT(2.*AI*ER1 )
      RM2 =SQRT(2.*AI*ER2 )
   10 R=RANF(0)
   50 VO2=(VOM**2)*R
      VO=SQRT(VO2)
   60 CONTINUE
      IF(MOM.LT.100) GO TO 100
      B2=VO2*A/3.14159
      GO TO 110
  100 B2=VO2*A/G**(4./MOM)
C
C     ROTATOR MODEL
C
C     TRANDITION PROBABILITY FOR ROTATOR 1
C     TRANSITION PROBABILITY FOR ROTATOR 2
  110 CONTINUE
      BB=SQRT(B2)
      L10=I1+0.1
```

```
      L20=I2+0.1
  120 R=RANF(0)
C     SEE PROB. STATEMENT NO. 600
      RRRR=R
      CALL LINKMC(L10,L20,BB,ETR)
      JJ1=J1FIN
      JJ2=J2FIN
  130 J1=2*JJ1-2+MOD(L10,2)
      J2=2*JJ2-2+MOD(L20,2)
C
C     ************************************
C
      ER1P=4.0241E-16*J1*(J1+1)
      ER2P=4.0241E-16*J2*(J2+1)
  200 GP2=(G2-4.*(ER1P+ER2P-(ER1+ER2))/W)
      IF(GP2.LT.0.0) GO TO 150
      GO TO 160
  150 IF (KGP.GE.1) RETURN
      KGP=KGP+1
      GO TO 10
  160 GP=SQRT(GP2)
      RM1P=SQRT(2.*AI*ER1P)
      RM2P=SQRT(2.*AI*ER2P)
  205 BP=(G*BB+2.*(RM1+RM2-RM1P-RM2P)/W)/GP
      IF(BP.LT.0.0) GO TO 10
      GO TO 210
  700 G2=G*G
  701 R=RANF(0)
      EPS=6.28318*R
  710 R=RANF(0)
  750 VO2=(VOM**2)*R
      VO=SQRT(VO2)
  760 CONTINUE
      IF(MOM.LT.100) GO TO 800
      B2=VO2*A/3.14159
      GO TO 810
  800 B2=VO2*A/G**(4./MOM)
  810 CONTINUE
      BB=SQRT(B2)
  860 GP=G
  905 BP=BB
      J1=I1+.001
      J2=I2+.001
  210 IF (MOM.LT.100)  GO TO 220
      VOP=BP*POA
```

```
      IF(VOP.GT..99995) VOP=.99995
      GO TO 230
  220 VOP=BP*GP**(2./MOM)/SQRT(A)
  230 XI=SCATER(VO,MOM)
      XIP=SCATER(VOP,MOM)
  250 XIB=.5*(XI+XIP)
  260 GX=U2-U1
      GY=V2-V1
      GZ=W2-W1
  300 CE=COS(EPS)
      SE=SIN(EPS)
      CX=COS(XIB)
      SX=SIN(XIB)
      GPG=GP/G
  350 RTG=SQRT(G2-GX**2)
      GPX=GPG*(GX*CX-RTG*SX*CE)
      GPY=GPG*(GY*CX+(GX*GY*CE+G*GZ*SE)/RTG*SX)
      GPZ=GPG*(GZ*CX+(GX*GZ*CE-G*GY*SE)/RTG*SX)
  400 U2=.5*(U1+U2+GPX)
      V2=.5*(V1+V2+GPY)
      W2=.5*(W1+W2+GPZ)
      U1=U2-GPX
      V1=V2-GPY
      W1=W2-GPZ
  460 I1=J1
      I2=J2
      RETURN
      END

*DECK LINK$$
      SUBROUTINE LINKMC(I1,I2,BB,ETR)
      DIMENSION PWAVE(20,20),LABCSA(16)
      COMMON /CM1/ PWAVE,EKIN,L10,L20,BIMP,NMAX,NPRINT,L1PAR,L2PAR
      COMMON /CM2/ JEL1,JEL2,LABCSA,LLMAX,ISELCT
      COMMON /CM3/ VA,VB,IPRT1,IPRT2,IPRT3,IPRT4
      COMMON /CMVR1/ VC,VALPHA,VC6,BBIMP,EEEE
C**   INPUT  **  SELECTION FOR OUTPUT (0 FOR PWAVE/1 FOR P)
      ISELCT=1
C**   INPUT  **  MIN PROBABILITY
C**   INPUT **  INITIAL ROTATIONAL STATES
      L10=I1
      L20=I2
C**   INPUT **  RELATIVE KINETIC ENERGY (IN EV)     EKIN= ETR/1.602E-12
      EKIN=ETR*.6242197E+12
C**   INPUT **  IMPACT PARAMETER (IN ANGSTROM)
```

```
      BIMP=BB*1.E08
C**   INPUT **  MAX NO. OF TERMS IN EXP
      NMAX= 80
C**   INPUT ** INDEX FOR PRINT OUT
      IPRT1= 1
      IPRT2= 1
      IPRT3= NMAX+1
      IPRT4= 0
C**   INPUT **  POTENTIAL PARAMETERS FOR SPHERICAL PART
C**           V(R)= VC*EXP(-VALPHA*R)-VC6/R**6
C**           V IN EV, R IN ANGSTROM
      VC=3440.
      VALPHA=3.160
      VC6=73.40
C**   INPUT **  POTENTIAL PARAMETERS FOR NON-SPHERICAL PART
      VA=.2
      VB=.2
      JMAX= 20
 5010 CONTINUE
      DO 5016 I=1,JMAX
      DO 5016 J=1,JMAX
      PWAVE(I,J)= 0.0
 5016 CONTINUE
C******** NPRINT
      NPRINT= NMAX
      IF(EKIN.LE.0.001) EKIN= 0.001
      IF(EKIN.GE.0.5) EKIN= 0.5
      CALL PROB
 5999 CONTINUE
      RETURN
      END

*DECK PROB$$
      SUBROUTINE PROB
      COMMON/PRBOUT/PSUM(400),RRRR,J1FIN,J2FIN
      COMMON /MV1/ AMATRX(20,20,9)
      COMMON /MV2/ VBB,VAA,BROT,ETOT,BRC,VVALP
      COMMON /CMVR1/ VC,VALPHA,VC6,BIMP,EEEE
      COMMON /MV3/ NCOUNT
      COMMON /CM1/ PWAVE,EKIN,L10,L20,BBBB,NMAX,NPRINT,L1PAR,L2PAR
      COMMON /CM2/ JEL1,JEL2,LABCSA,LLMAX,ISELCT
      COMMON /CM3/ VA,VB,IPRT1,IPRT2,IPRT3,IPRT4
      DIMENSION PWAVEC(20,20)
      DIMENSION PODD(20,20),PEVN(20,20),PWAVE(20,20)
      DIMENSION AKSUM0(20,20),AKSUM1(20,20)
```

```
      DIMENSION LABCSA(16)
      TCLOCK= 0
      BIMP=BBBB
      JMAX=20
      LMAX= 2*JMAX-2
C*********  REDUCED MASS
      RMASS= 14.02
C*********  ROTATIONAL CONSTANT
      BROT= 0.2512E-3
      VVALP= 0.045723*VALPHA/ SQRT(RMASS)
      VAA= 0.4472136*VA
      VBB= 0.2*VB*0.6298283
      ETOT= EKIN+ FLOAT(L10*(L10+1)+L20*(L20+1))*BROT
      EB= ETOT/BROT
      EB1= SQRT(EB)
      LLMAX= INT(EB1)+1
C*****  PRINT  901-1
   11 CONTINUE
      IF(LLMAX.GT.LMAX) LLMAX=LMAX
      DO 18 I=1,JMAX
      DO 18 J=1,JMAX
      PEVN(I,J)= 0.0
      PODD(I,J)= 0.0
      PWAVE(I,J)= 0.0
      PWAVEC(I,J)= 0.0
      AKSUM0(I,J)=0.0
      AKSUM1(I,J)= 0.0
      DO 16 M=1,9
      AMATRX(I,J,M)= 0.0
   16 CONTINUE
   18 CONTINUE
      LL10= L10+1
      LL20= L20+1
      JEL1= (LL10+1)/2
      JEL2=(LL20+1)/2
      L1PAR= MOD(L10,2)+1
      L2PAR= MOD(L20,2)+1
      CLO= FLOAT((2*L10+1)*(2*L20+1))
      PEO= 0.0
C*********  N= 1
      N=1
      LL1I= LL10
      LL2I= LL20
      NCOUNT= 0
      DO 59 K=1,9
```

```
      CALL VMATRX(LL1I,LL2I,K)
   50 CONTINUE
      LL1FMN= MAXO(LL10-2,L1PAR)
      LL1FMX= LL10+2
      LL2FMN= MAXO(LL20-2,L2PAR)
      LL2FMX= LL20+2
      K= 1
      JJI1= (LL1I+1)/2
      JJI2= (LL2I+1)/2
      DO 64 I=1,3
      LL2F= LL20-4+2*I
      DO 63 J=1,3
      LL1F= LL10-4+2*J
      IF(LL2F.LT.1.OR.LL1F.LT.1) GO TO 62
      JJF1= (LL1F+1)/2
      JJF2= (LL2F+1)/2
      AKSUM0(JJF1,JJF2)= AMATRX(JJI1,JJI2,K)
   62 K=K+1
   63 CONTINUE
   64 CONTINUE
      TOTPW= 0.0
      DO 74 LL1F=LL1FMN,LL1FMX,2
      DO 73 LL2F=LL2FMN,LL2FMX,2
      JJF1= (LL1F+1)/2
      JJF2= (LL2F+1)/2
      PODD(JJF1,JJF2)= AKSUM0(JJF1,JJF2)
      PEVN(JJF1,JJF2)= 0.0
      IF(LL1F.EQ.LL1I.AND.LL2F.EQ.LL2I) PEVN(JJF1,JJF2)=1.0
      PWAVE(JJF1,JJF2)= PODD(JJF1,JJF2)**2*4.0+PEVN(JJF1,JJF2)**2
      P=PWAVE(JJF1,JJF2)
      L01=LL1F-1
      L02=LL2F-1
C*****  PRINT  902-1
   72 CONTINUE
      TOTPW=TOTPW+P
   73 CONTINUE
   74 CONTINUE
C*****  PRINT  904-1
   75 CONTINUE
      IF(NMAX.EQ.1) GO TO 300
      N= 2
C*********100
  100 CONTINUE
      NCOUNT= 0
      N2= 2*N-2
```

```
      LL2IMN=MAX0(LL20-N2,L2PAR)
      LL2IMX= LL20+N2
      IF(LL2IMX.GE.LLMAX) LL2IMX= LLMAX
      DO 149 LL2I=LL2IMN,LL2IMX,2
      JJI2= (LL2I+1)/2
      EB2= SQRT(EB- FLOAT(LL2I-1)**2)
      LLMAX1= INT(EB2)+1
      LL1I=LL10+N2
      JJI1=(LL1I+1)/2
      IF(LLMAX1.GE.LMAX) LLMAX1= LMAX
      IF(LL1I.GT.LLMAX1) GO TO 130
      DO 114 K=5,8,3
      CALL VMATRX(LL1I,LL2I,K)
  114 CONTINUE
      DO 119 K=3,9,3
      CALL VMATRX(LL1I,LL2I,K)
  119 CONTINUE
      IF(LL1I-2.LT.1) GO TO 125
      AMATRX(JJI1,JJI2,4) = AMATRX(JJI1-1,JJI2,6)
      K=4
      IF(LL2I.EQ.LL20-N2.OR.LL2I.EQ.LL20+N2)  CALL VMATRX(LL1I,LL2I,K)
      AMATRX(JJI1,JJI2,7)= AMATRX(JJI1-1,JJI2+1,3)
      K= 7
      IF(LL2I.EQ.LL20+N2-2.OR.LL2I.EQ.LL20+N2) CALL VMATRX(LL1I,LL2I,K)
      IF(LL2I-2.LT.1) GO TO 130
      AMATRX(JJI1,JJI2,1)= AMATRX(JJI1-1,JJI2-1,9)
      K= 1
      IF(LL2I.EQ.LL20-N2+2.OR.LL2I.EQ.LL20-N2) CALL VMATRX(LL1I,LL2I,K)
  125 CONTINUE
      IF(LL2I-2.LT.1) GO TO 130
      AMATRX(JJI1,JJI2,2) = AMATRX(JJI1,JJI2-1,8)
      K= 2
      IF(LL2I.EQ.LL20-N2)  CALL VMATRX(LL1I,LL2I,K)
  130 CONTINUE
      LL1I=LL10-N2
      JJI1= (LL1I+1)/2
      IF(LL1I.LT.L1PAR) GO TO 149
      DO 134 K=5,8,3
      CALL VMATRX(LL1I,LL2I,K)
  134 CONTINUE
      DO 139 K=1,7,3
      CALL VMATRX(LL1I,LL2I,K)
  139 CONTINUE
      AMATRX(JJI1,JJI2,6)= AMATRX(JJI1+1,JJI2,4)
      K= 6
```

```
      IF(LL2I.EQ.LL20-N2.OR.LL2I.EQ.LL20+N2)  CALL VMATRX(LL1I,LL2I,K)
      AMATRX(JJI1,JJI2,9)= AMATRX(JJI1+1,JJI2+1,1)
      K=9
      IF(LL2I.EQ.LL20+N2-2.OR.LL2I.EQ.LL20+N2) CALL VMATRX(LL1I,LL2I,K)
      IF(LL2I-2.LT.1) GO TO 149
      AMATRX(JJI1,JJI2,2)= AMATRX(JJI1,JJI2-1,8)
      K= 2
      IF(LL2I.EQ.LL20-N2) CALL VMATRX(LL1I,LL2I,K)
      AMATRX(JJI1,JJI2,3)= AMATRX(JJI1+1,JJI2-1,7)
      K= 3
      IF(LL2I.EQ.LL20-N2+2.OR.LL2I.EQ.LL20-N2) CALL VMATRX(LL1I,LL2I,K)
  149 CONTINUE
C*********  150
      LL1IMN= MAX0(LL10-N2+2,L1PAR)
      LL1IMX= LL10+N2-2
      IF(LL1IMX.GE.LLMAX)LL1IMX= LLMAX
      DO 199 LL1I=LL1IMN,LL1IMX,2
      JJI1= (LL1I+1)/2
      EB2= SQRT(EB- FLOAT(LL1I-1)**2)
      LLMAX1=INT(EB2)+1
      LL2I= LL20+N2
      JJI2= (LL2I+1)/2
      IF(LLMAX1.GE.LMAX) LLMAX1= LMAX
      IF(LL2I.GT.LLMAX1) GO TO 180
      DO 164 K=5,9
      IF(LL1I.EQ.LL10+N2-2.AND.K.EQ.6) GO TO 163
      CALL VMATRX(LL1I,LL2I,K)
      GO TO 164
  163 CONTINUE
      AMATRX(JJI1,JJI2,6)= AMATRX(JJI1+1,JJI2,4)
  164 CONTINUE
      IF(LL2I-2.LT.1) GO TO 175
      AMATRX(JJI1,JJI2,2)= AMATRX(JJI1,JJI2-1,8)
      AMATRX(JJI1,JJI2,3)= AMATRX(JJI1+1,JJI2-1,7)
      IF(LL1I-2.LT.1) GO TO 180
      AMATRX(JJI1,JJI2,1)= AMATRX(JJI1-1,JJI2-1,9)
  175 CONTINUE
      IF(LL1I-2.LT.1) GO TO 180
      AMATRX(JJI1,JJI2,4)= AMATRX(JJI1-1,JJI2,6)
  180 CONTINUE
      LL2I=LL20-N2
      JJI2= (LL2I+1)/2
      IF(LL2I.LT.L2PAR) GO TO 199
      DO 184 K=5,6
      IF(LL1I.EQ.LL10+N2-2.AND.K.EQ.6) GO TO 183
```

```
      CALL VMATRX(LL1I,LL2I,K)
      GO TO 184
  183 CONTINUE
      AMATRX(JJI1,JJI2,6)= AMATRX(JJI1+1,JJI2,4)
  184 CONTINUE
      DO 189 K=1,3
      CALL VMATRX(LL1I,LL2I,K)
  189 CONTINUE
      AMATRX(JJI1,JJI2,8)= AMATRX(JJI1,JJI2+1,2)
      AMATRX(JJI1,JJI2,9)= AMATRX(JJI1+1,JJI2+1,1)
      IF(LL1I-2.LT.1) GO TO 199
      AMATRX(JJI1,JJI2,4)= AMATRX(JJI1-1,JJI2,6)
      AMATRX(JJI1,JJI2,7)= AMATRX(JJI1-1,JJI2+1,3)
C*********  199
  199 CONTINUE
      LL1FMX=LL10+2*N
      LL2FMX= LL20+2*N
      LL1FMN= LL10-2*N
      IF(LL1FMN.LT.L1PAR) GO TO 201
      LL11=LL1FMN+2
  200 CONTINUE
      LL2FMN=LL20-2*N
      IF(LL2FMN.LT.L2PAR) GO TO 202
      LL22= LL2FMN+2
      GO TO 205
  201 CONTINUE
      LL1FMN= L1PAR
      LL11= L1PAR
      GO TO 200
  202 CONTINUE
      LL2FMN=L2PAR
      LL22= L2PAR
  205 CONTINUE
      LL22F= LL2FMX-2
      IF(LL2FMX.LE.LLMAX) GO TO 206
      LL2FMX=LLMAX
      LL22F= LLMAX
  206 CONTINUE
      DO 249 L2=LL22,LL22F,2
      LL11F= LL1FMX-2
      EB2= SQRT(EB- FLOAT(L2-1)**2)
      LLMAX1= INT(EB2)+1
      IF(LLMAX1.GE.LMAX) LLMAX1= LMAX
      IF(LL1FMX.GE.LLMAX1) LL11F= LLMAX1
      DO 248 L1= LL11,LL11F,2
```

```
      K1= 1
      K2= 0
      L22=L2-2
      L11= L1-2
      IF(L2.LE.L2PAR) L22= L2PAR
      IF(L1.LE.L1PAR) L11= L1PAR
      IF(L2.LE.L2PAR) K1=4
      IF(L1.LE.L1PAR) K2= 1
      K= K1
      J1= (L1+1)/2
      J2= (L2+1)/2
      AK= AKSUM0(J1,J2)
      L2P2=L2+2
      DO 219 LL2= L22,L2P2,2
      K= K+K2
      L1P2=L1+2
      DO 218 LL1=L11,L1P2,2
      JJ1= (LL1+1)/2
      JJ2= (LL2+1)/2
      AKSUM1(JJ1,JJ2)= AK*AMATRX(J1,J2,K)+AKSUM1(JJ1,JJ2)
      K= K+1
  218 CONTINUE
  219 CONTINUE
C********  PRINT OF AMATRX
  220 CONTINUE
  248 CONTINUE
  249 CONTINUE
C********  250
      LL1FMX= LL10+2*N
      TOTPC= 0.0
      TOTPW= 0.0
      DO 299 LL2F=LL2FMN,LL2FMX,2
      LL11F= LL1FMX
      FB2= SQRT(FB- FLOAT(LL2F-1)**2)
      LLMAX1= INT(FB2)+1
      IF(LLMAX1.GE.LMAX) LLMAX1= LMAX
      IF(LL1FMX.GE.LLMAX1) LL11F= LLMAX1
      DO 298 LL1F=LL1FMN,LL11F,2
      JJF1= (LL1F+1)/2
      JJF2= (LL2F+1)/2
      AKSUM1(JJF1,JJF2)= AKSUM1(JJF1,JJF2)/ FLOAT(N)
      IF(MOD(N,2).NE.0) GO TO 294
      AKSUM1(JJF1,JJF2)= -4.0*AKSUM1(JJF1,JJF2)
      PEVN(JJF1,JJF2)= PEVN(JJF1,JJF2)+ AKSUM1(JJF1,JJF2)
      PWAVE(JJF1,JJF2)= PODD(JJF1,JJF2)**2*4.0+PEVN(JJF1,JJF2)**2
```

```
      GO TO 295
  294 CONTINUE
      PODD(JJF1,JJF2)= PODD(JJF1,JJF2)+ AKSUM1(JJF1,JJF2)
      PWAVE(JJF1,JJF2)= PODD(JJF1,JJF2)**2*4.0+PEVN(JJF1,JJF2)**2
  295 CONTINUE
      P= PWAVE(JJF1,JJF2)
      LO1= LL1F-1
      LO2= LL2F-1
C********* PRINT OF PWAVE
  296 CONTINUE
C*****  PRINT  902-2
  297 CONTINUE
      TOTPW= TOTPW+P
      AKSUM0(JJF1,JJF2)= AKSUM1(JJF1,JJF2)
      AKSUM1(JJF1,JJF2)= 0.0
  298 CONTINUE
  299 CONTINUE
      PE1=PWAVE(JEL1,JEL2)
      PE10= ABS((PE1-PE0)/PE1)
C*****  PRINT  904-2
 3904 CONTINUE
      IF(ABS(TOTPW-1.0).LT.0.1E-3.AND.PE10.LT.0.1E-3) GO TO 300
      IF(N.EQ.NMAX) GO TO 300
      N=N+1
      PE0= PE1
      GO TO 100
  300 CONTINUE
C*********  ELASTIC
C*********  FINAL PRINT
      IF(IPRT4.EQ.1) GO TO 325
      MPRINT=0
      PMAX= 0.1E-5
  301 CONTINUE
C*****  PPINT  901-2
C*****  PPINT  910-1
      IMN= LL2FMN
      IMX=LL2FMX
      IF(MOD(LL2FMX-L2PAR,2).NE.0) IMX= LL2FMX-1
      DO 319 I=IMN,IMX,2
      LL2F= IMX+IMN-I
      J2= (LL2F+1)/2
      LL1F= LL1FMX
      EB2= SQRT(EB- FLOAT(LL2F-1)**2)
      LLMAX1= INT(EB2)+1
      IF(LLMAX1.GE.LMAX) LLMAX1= LMAX
```

```
      IF(LL1FMX.GE.LLMAX1) LL11F=LLMAX1
      J1MX= (LL11F+1)/2
      IF(J1MX.GT.16) J1MX=16
      L02=LL2F-1
C*****  PRINT  911-1
      IF(MPRINT.EQ.1) GO TO 319
      LMIN2= MIN0(L20,L02)
      CL10= FLOAT(2*LMIN2+1)
      J1MN=(L1PAR+1)/2
      DO 318 J1=J1MN,J1MX
      L01= 2*J1-3+L1PAR
      LMIN1= MIN0(L10,L01)
      CL1= CL10*FLOAT(2*LMIN1+1)
      P= PWAVE(J1,J2)
      PCORCT= CL1/CL0*P
      TOTPC=TOTPC+PCORCT
      PWAVEC(J1,J2)= PCORCT
      IF(J1.EQ.JEL1.AND.J2.EQ.JEL2) GO TO 318
      IF(ISELCT.EQ.0) POUT=P
      IF(ISELCT.EQ.1) POUT= PCORCT
  318 CONTINUE
  319 CONTINUE
      LABCSA(1)= L1PAR-1
      DO 320 I=2,16
      LABCSA(I)=LABCSA(1)+(I-1)*2
  320 CONTINUE
C*****  PRINT  912-1
C     IF(MPRINT.EQ.1) GO TO 9906
C*********  PRINT OF PCORCT WITH ELASTIC MODIFIED
  325 CONTINUE
      PC= 1.0-TOTPC+PWAVEC(JEL1,JEL2)
      PWAVEC(JEL1,JEL2)= PC
      IF(ISELCT.EQ.0) PSUM(1)=PWAVE(JEL1,JEL2)
      IF(ISELCT.EQ.1) PSUM(1)=PWAVEC(JEL1,JEL2)
C     STATISTIC MODIFICATION OF ELASTIC COLLISION
C     RRRR :    P(N)=P(N)-PSUM(1)/(1.-PSUM(1))  PBAR VS RRRR
  600 RRRR=(1.0-PSUM(1))*RRRR
C     IF(RRRR.GT.PSUM(1)) GO TO 1905
C     J1FIN=JEL1
C     J2FIN=JEL2
C     GO TO 2001
 1905 CONTINUE
      NN=1
      N=1
 1910 CONTINUE
```

```
      J1MN= JEL1-N
      IF(J1MN.LT.1) J1MN=1
      J1MX= JEL1+N
      IF(J1MX.GT.JMAX) J1MX= JMAX
      K=0
      J2=JEL2-N
      IF(J2.LT.1) GO TO 1942
 1920 CONTINUE
      DO 1940 J1= J1MN,J1MX
      NN=NN+1
      IF(ISELCT.EQ.1) PWAVE(J1,J2)= PWAVEC(J1,J2)
      CALL SUMP(J1,J2,NN)
C     IF(RRRR.GT.PSUM(NN)) GO TO 1940
      IF(RRRR.GT.(PSUM(NN)-PSUM(1))) GO TO 1940
      J1FIN=J1
      J2FIN=J2
      GO TO 2001
 1940 CONTINUE
      IF(K.EQ.1) GO TO 1950
 1942 K=1
      J2= JEL2+N
      IF(J2.GT.JMAX) GO TO 1950
      GO TO 1920
 1950 CONTINUE
      J2MN= JEL2-N+1
      IF(J2MN.LT.1) J2MN=1
      J2MX= JEL2+N-1
      IF(J2MX.GT.JMAX) J2MX= JMAX
      K= 0
      J1= JEL1-N
      IF(J1.LT.1) GO TO 1992
 1970 CONTINUE
      DO 1990 J2= J2MN,J2MX
      NN= NN+1
      IF(ISELCT.EQ.1)  PWAVE(J1,J2)= PWAVEC(J1,J2)
      CALL SUMP(J1,J2,NN)
C     IF(RRRR.LE.PSUM(NN)) GO TO 1985
      IF(RRRR.LE.(PSUM(NN)-PSUM(1))) GO TO 1985
      IF(ABS(1.0-PSUM(NN)).LT.1.0E-4) GO TO 1985
      IF(NN.GE.400) GO TO 1985
      GO TO 1990
 1985 CONTINUE
      J1FIN=J1
      J2FIN=J2
      GO TO 2001
```

```
 1990 CONTINUE
      IF(K.EQ.1) GO TO 2000
 1992 K=1
      J1= JEL1+N
      IF(J1.GT.JMAX) GO TO 2000
      GO TO 1970
 2000 CONTINUE
      N=N+1
      GO TO 1910
 2001 CONTINUE
 1000 CONTINUE
      RETURN
      END

*DECK SUM$$
      SUBROUTINE SUMP(J1,J2,NNN)
      COMMON/PRBOUT/PSUM(400),RRRR,J1FIN,J2FIN
      COMMON/CM1/ PWAVE,EKIN,L10,L20,BBBB,NMAX,NPRINT,L1PAR,L2PAR
      DIMENSION PWAVE(20,20)
      N=NNN
      PSUM(N)= PSUM(N-1)+PWAVE(J1,J2)
      RETURN
      END

*DECK VMAT$$
      SUBROUTINE VMATRX(LL1,LL2,K)
C*****  REVISED FOR ROOT
      COMMON /MV1/ AMATRX(20,20,9)
      COMMON /MV2/ VBB,VAA,BROT,ETOT,BRC,VVALP
      COMMON /CMVR1/ VC,VALPHA,VC6,BIMP,EIJ
      COMMON /MV3/ NCOUNT
      COMMON/CV1/ABCC(40,40,9)
      L1J= LL1-1
      L2J= LL2-1
      IF(K.GT.3) GO TO 1011
      L2I= L2J-2
      IF(L2I.LT.0) GO TO 1510
      GO TO 1100
 1011 IF(K.GT.6) GO TO 1012
      L2I= L2J
      GO TO 1100
 1012 L2I= L2J+2
 1100 CONTINUE
      IF(MOD(K,3).NE.1) GO TO 1111
      L1I= L1J-2
```

```
      IF(L1I.LT.0) GO TO 1510
      GO TO 1200
 1111 IF(MOD(K,3).NE.2) GO TO 1112
      L1I= L1J
      GO TO 1200
 1112 L1I= L1J+2
 1200 CONTINUE
      ABC= ABCC(LL1,LL2,K)
      IF(ABC.NE.0.0) GO TO 1299
CALCULATION OF VEFF(L1I,L2I / L1J,L2J )
      CC1= CG2O(L1I,L1J)
      CC2= CG2O(L2I,L2J)
      IF(K.LE.5) CSIGN= (-1.0)**(L1J+L2J)
      IF(K.GE.6) CSIGN= (-1.0)**(L1I+L2I)
      C=  FLOAT((2*L1I+1)*(2*L2I+1)*(2*L1J+1)*(2*L2J+1))**0.25*CSIGN
      B= VBB*CC1*CC2
      A=0.0
      IF(L2I.NE.L2J) GO TO 1215
      A= VAA*CC1/ SQRT( FLOAT(2*L2I+1))
      IF(MOD(L2I,2).NE.0) A=-A
 1215 IF(L1I.NE.L1J) GO TO 1219
      AA= VAA*CC2/ SQRT( FLOAT(2*L1I+1))
      IF(MOD(L1I,2).NE.0) AA=-AA
      A= A+AA
 1219 CONTINUE
      ABC= C*(B+A)
      ABCC(LL1,LL2,K)= ABC
 1299 CONTINUE
      WI= BROT* FLOAT(L1I*(L1I+1)+L2I*(L2I+1))
      WJ=BROT* FLOAT(L1J*(L1J+1)+L2J*(L2J+1))
      WIJ= ABS(WI-WJ)
      EI= ETOT-WI
      EJ=ETOT-WJ
      IF(EI.LE.0.0.OR.EJ.LE.0.0) GO TO 1510
      EIJ= 0.5*(EI+EJ)
      CALL ROOT(RC)
      BRC= 1.0-(BIMP/RC)**2+VC6/EIJ/RC**6
      EIJ1= EIJ*BRC
      IF(K.EQ.5) GO TO 1500
      IF(L1I.EQ.L2J.AND.K.EQ.3) GO TO 1500
      IF(L1I.EQ.L2J.AND.K.EQ.7) GO TO 1500
      AIJ= VVALP* SQRT(EIJ1)/WIJ
      EW= EIJ1/WIJ
      DBALPH= EW/AIJ
      APAI= 1.570796327/AIJ
```

```
      F= EXP(-APAI)
      FAIJ= 2.0*APAI*F/(1.0-F*F)
      AAA= ABC*DBALPH*FAIJ
 1498 CONTINUE
C***  999  CHECK PRINT
  999 CONTINUE
      NCOUNT= NCOUNT+1
 1499 CONTINUE
      JJ1= (LL1+1)/2
      JJ2= (LL2+1)/2
      AMATRX(JJ1,JJ2,K)= AAA
      RETURN
 1500 CONTINUE
      AAA= ABC/VVALP* SQRT(EIJ1)
      GO TO 1498
 1510 CONTINUE
      AAA= 0.0
      GO TO 1499
      END
*DECK CG$$
      FUNCTION CG20(J1,J2)
C     DOUBLE PRECISION FUNCTION CG20(J1,J2)
      IF(J2.EQ.J1+2.OR.J2.EQ.J1-2) GO TO 8001
      IF(J2.EQ.J1) GO TO 8002
      C= 0.0
      GO TO 8100
 8001 CONTINUE
      IF(J2.EQ.J1+2) J=J1
      IF(J2.EQ.J1-2) J=J2
      X1=  FLOAT(J+2)/ FLOAT(2*J+5)
      X2=  FLOAT(J+1)/ FLOAT(2*J+3)
      X3= 1.0/ FLOAT(2*J+1)
      C=  SQRT(1.5*X1*X2*X3)
      GO TO 8099
 8002 CONTINUE
      J= J1
      X1=  FLOAT(J+1)/ FLOAT(2*J+3)
      X2=  FLOAT(J)/ FLOAT(2*J+1)
      X3= 1.0/ FLOAT(2*J-1)
      C= - SQRT(X1*X2*X3)
 8099 IF(MOD(J,2).NE.0) C= -C
 8100 CG20=C
      RETURN
      END
```

```
*DECK ROO$$
      SUBROUTINE ROOT(RC)
C*****  REVISED  8/26/74
      COMMON /CMVR1/ VC,VALPHA,VC6,BIMP,EKIN
      RMIN= 1.12
      RRO= ALOG(VC/EKIN)/VALPHA
      IF(RRO.GE.4.1) RRO= 4.1
      N=1
 3099 CONTINUE
      RR=RRO
 3100 CONTINUE
      RL= EKIN*BIMP**2/RR**2
      V= VC* EXP(-VALPHA*RR)
      V1= -VALPHA*V
      IF(VC6.EQ.0.0) GO TO 3101
      VR= VC6/RR**6
      V= V-VR
      V1= V1+6.0*VR/RR
 3101 CONTINUE
      F= (V+RL-EKIN)/(2.0*RL/RR-V1)
      IF(ABS(F/RR).LT.0.1E-5) GO TO 3199
      IF(N.GE.100) GO TO 3299
      RR= RR+F
      IF(RR.LT.RMIN) GO TO 3900
      N=N+1
      GO TO 3100
 3199 CONTINUE
      RC= RR
      RETURN
 3299 CONTINUE
      WRITE(6,998) RR,F,RRO
  998 FORMAT(1H0//5X,14HERROR N GT 100,3X,3HRR=E13.5,3X,2E13.5//)
      RR=RRO
      GO TO 3199
 3900 CONTINUE
      RRO= 0.5*(RRO+RMIN)
      GO TO 3099
      END

*DECK OUT$$
      SUBROUTINE OUTPUT(M)
      COMMON /TIME/ TO,TS,TF,TM,DTO,DTM,TN
      COMMON /CV/ MAX,MAX6,C1,RHO1
      COMMON /CONST/ W,A,VOM,SF,CO
      COMMON /RANDOM/ R
```

```
      COMMON /ANSWER/ MOM,T(4),G,DVOL,AI,POA,ROT1
      COMMON /PART/ P(5001)
      COMMON /CV1/ABCC(40,40,9)
      DIMENSION FC(40),FW(40)
C
      NTM=(TM-DTM)/DTO+.5
      TAUBAR=0.1*NTM*DTO/DTM
      COC=T(2)/(T(1)*C1)*.886227
      COC2=T(3)/(T(1)*1.5*C1*C1)
      EOE=.80482E-15*T(4)/(T(1)*W*C1*C1)
      WRITE(6,600) COC,COC2,EOE,TAUBAR
      DO 100 I=1,40
      FC(I)=0
  100 FW(I)=0
      COE=1.0/C1
      DO 200 I=5,MAX6,5
      JC=P(I)*COE*10. +1
      JW=P(I+1)+1.01
      IF(JC.GT.40) JC=40
      IF(JW.GT.40) JW=40
      FC(JC)=FC(JC)+1.
      FW(JW)=FW(JW) +1.
  200 CONTINUE
      DO 300 I=1,40
      FC(I)=FC(I)/MAX
  300 FW(I)=FW(I)/MAX
  600 FORMAT( 5HOCOC=G13.6,1X6HCOC2 = G13.6,1X6HEOE = G13.6,
     11X7HTAUBAR= F5.1)
C
C     THIS IS TO PLOT FC AND FW
      WRITE(10) TAUBAR,NTM,MAX,COC2,EOE,FC,FW
C
C     THESE CARDS ARE FOR RESTART PROGRAM  TIL NEXT  *** MARKS
      WRITE(9) MOM,T,G,DVOL,W,A,VOM,SF,CO,TO,TS,TF,TM,DTO,DTM,TN,MAX,
     1MAX6,C1,RHO1,P,AI,ROT1,POA,ABCC,R
      END FILE 9
      REWIND 9
C     ***  END OF THE  RESTART PROGRAM
      RETURN
      END

*DECK X2$$
      SUBROUTINE X2DIST(IROT)
      COMMON /RANDOM/ R
      COMMON/INITX2/ ERO
```

```
C
C       TO DETERMINE THE ROTATIONAL FREQUENCY(OM) FROM THE
C       X2-DISTRIBUTION(KAI-SQUARE)
C
C       IROT=  1.*SQRT(.25-2.48503E15*ERO*ALOG(1-R))-.5+.5 FOR 1 JUMP
C       IROT= .50*SQRT(.25-2.48503E15*ERO*ALOG(1-R))-.25+.5 FOR EVEN JUMP
C       IROT=2*I
C  10 R=RANF(0)
C       IROT=  1.*SQRT(.25-2.48503E15*ERO*ALOG(1.-R)) -.1666
C       RETURN
C       END

*DECK SCA$$
        FUNCTION SCATER(VO,MOM)
C       IF(VO.GE.0.0) SCATER=2.*ACOS(VO)
C       IF(VO.LT.0.0) SCATER=2.*(3.1415926+ACOS(-VO))
        SCATER=2.*ACOS(VO)
        RETURN
        END

*DECK MOM$$
        SUBROUTINE MOMENT
        COMMON /CV/ MAX,MAX6,C1,RHO1
        COMMON /ANSWER/ MOM,T(4),G,DVOL,AI,POA,ROT1
        COMMON /PART/ P(5001)
C
C       COMPUTES DESIRED MOMENTS
C
        DO 200 I=1,MAX
        LU=5*I-3
        T(1)=T(1)+1
        T(2)=T(2)+P(LU+3)
        T(3)=T(3)+P(LU+3)**2
        T(4)=T(4)+P(LU+4)**2+P(LU+4)
  200 CONTINUE
        RETURN
        END


C
C
C       SAMPLE INPUT DATA
C
"
C F(G/GM)-SELCT, ISELCT=1,C=0.4310,PC=0
```

```
1000
          .126472E-243632.933 .46519E-22.44272E-141.0          100
3.0    E-110.0          1.          11.
1.09    E-83.33    E-1
"
"
=
```

REFERENCES

1. Deiwert, George S.: Reflection of a Shock Wave From a Thermally Accommodating Wall; Molecular Simulation. Phys. Fluids, vol. 16, no. 8, Aug. 1973, pp. 1215-1219.

2. Bird, G. A.: Approach to Transitional Equilibrium in a Rigid Sphere Gas. Phys. Fluids, vol. 6, no. 10, Oct. 1963, pp. 1518-1519.

3. Bird, G. A.: Direct Simulation Monte Carlo Method - Current Status and Methods, pp. 85-93; The Formation and Deflection of Shock Waves, pp. 301-311. In Rarefied Gas-Dynamics; Proc. Sixth Internatl. Symp., 1968; Academic Press, N. Y., 1969.

4. Deiwert, George S.; and Yoshikawa, K. K.: Analysis of a Semiclassical Model for Rotational Transition Probabilities. Phys. Fluids, vol. 18, no. 9, Sept. 1975, pp. 1085-1088.

5. Yoshikawa, K. K.; and Itikawa, Y.: Monte Carlo Calculations of Diatomic Molecule Gas Flows including Rotational Mode Excitation. NASA TN D-8100, Jan. 1976.

6. Bird, G. A.: Numerical Simulation and the Boltzmann Equation. In Rarefied Gas-Dynamics; Proc. Seventh Internatl. Symp., 1970.

7. Hirschfelder, Joseph O.; Curtiss, Charles F.; and Bird, R. Byron: Molecular Theory of Gases and Liquids. John Wiley & Sons, Inc., N. Y., 1954.

8. Parker, J. G.: Rotational and Vibrational Relaxation in Diatomic Gases. Phys. Fluids, vol. 2, no. 4, July-Aug. 1959, pp. 449-462.

9. Lordi, John A.; and Mates, Robert E.: Rotational Relaxation in Nonpolar Diatomic Gases. Phys. Fluids, vol. 13, no. 2, Feb. 1970, pp. 291-308.

10. Pearson, W. E.; and Hansen, C. F.: Collision Induced Rotational Transition Probabilities in Diatomic Molecules. In Rarefied Gas-Dynamics; Proc. Eighth Internatl. Symp. 1972; Academic Press, N. Y., 1974, pp. 167-175.

11. Rabitz, H.: Rotational Energy Relaxation in Molecular Hydrogen, Jour. of Chem. Physics, vol. 63, no. 8, Oct. 1975.

12. Yoshikawa, K. K.; and Lee, K. L.: Collision Crossections for a Central Field Potential Function. ISAS RN-46, Univ. of Tokyo, 1977.

13. Vincenti, Walter G.; and Kruger, Charles H., Jr.: Introduction to Physical Gas Dynamics. John Wiley & Sons, Inc., 1965.

14. Rabitz, Herschel: Effective Potentials in Molecular Collisions. J. Chem. Phys., vol. 57, no. 4, Aug. 15, 1972, pp. 1718-1725.

15. Takayanagi, Kazuo: The Theory of Collisions Between Two Diatomic Molecules. Progr. Theor. Phys., vol. 11, no. 6, June 1954, pp. 557-594.

16. Levine, R. D.; and Bernstein, R. B.: Molecular Reaction Dynamics. Oxford Univ. Press, 1974.

17. Mark, Hans; and Paulissen, George T.: Electric Excitation of Certain Rare-Earth Nuclei by Protons. The Physical Review, vol. 100, no. 3, pp. 813-822, Nov. 1955.

18. Polanyi, J. C.; and Woodall, K. B.: Mechanism of Rotational Relaxation. Jour. of Chem. Physics, vol. 56, no. 4, Feb. 1972.

TABLE I.- INITIAL DISTRIBUTIONS AND FLOW CORRELATION

Figure	Velocity[a]	Rotational[a]	Energy partition	Temperature	Remarks
1a & b	$f_t=f_{tm}(T)$	$f_r=f_{rm}(T)$	$E_t/E_r=3/2$	$T=T_e$	Uniform flow
2a & b	$f_t\neq f_{tm}$	f_r=frozen	- - -	- - -	- - -
3	$f_t=f_{tm}(T_t)$	$f_r\neq f_{rm}$	$E_t/E_r=3/2$	$T_t=T_e$	Sound absorption experiment
4	$f_t=f_{tm}(T_t)$	$f_r=f_{rm}(T_r)$	$E_t/E_r>>3/2$	$T_t>>T_e>>T_r=0$	Shock wave
5a & b	$f_t=f_{tm}(T_t)$	$f_r=f_{rm}(T_r)$	$E_t/E_r<<3/2$	$T_t<<T_e<<T_r$	Free-jet expansion
6a & b	$f_t=f_{tm}(T_t)$	$f_r\neq f_{rm}$	$E_t/E_r<<3/2$	$T_t<<T_e$	Chemical-fluorescence experiment

[a] $f_{tm}(T)$ and $f_{rm}(T)$ denote translational and rotational Maxwell-Boltzmann distributions with temperature T.

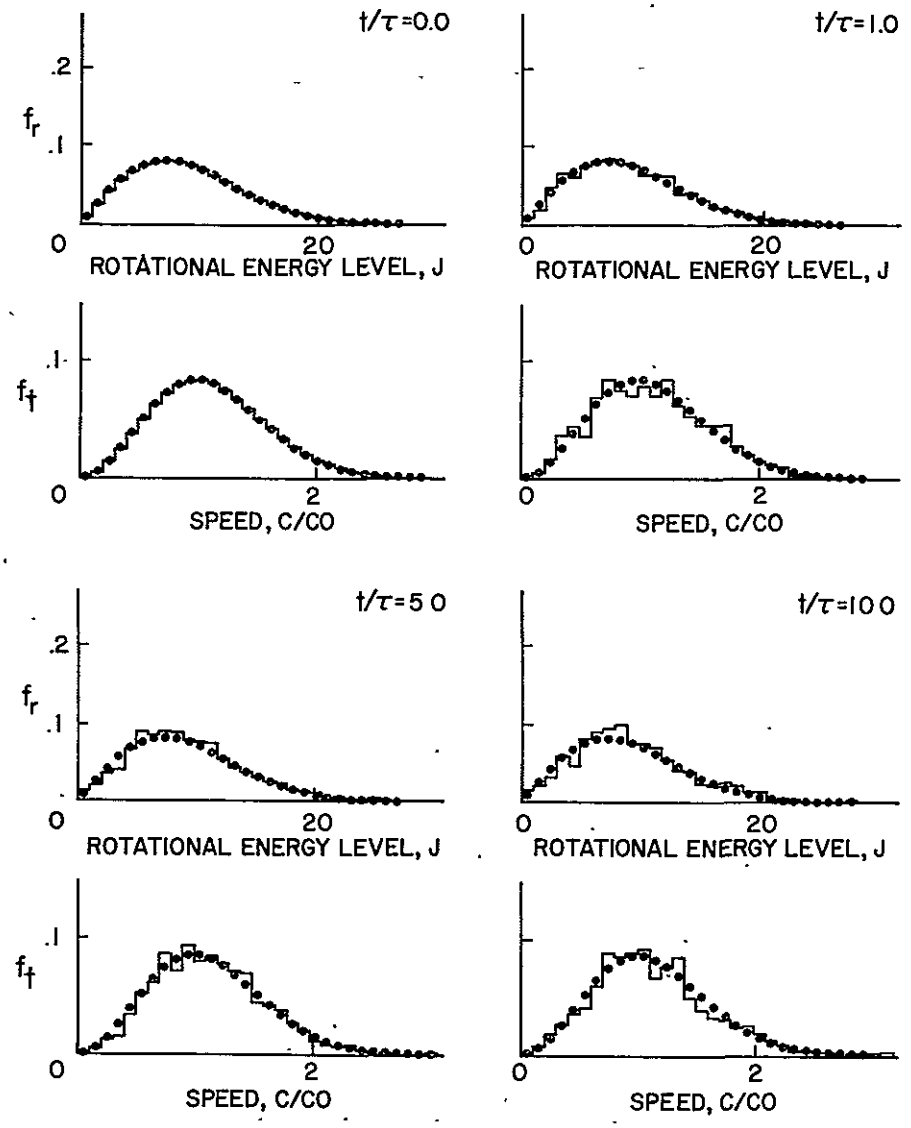

(a) Monte Carlo Results: $f_t(0,x)$ = Maxwellian where $x = c/c_0$; $f_r(0,j)$ = Boltzmann; $T_t = T_r = 320$ K.

Figure 1.- Distribution functions for complete equilibrium.

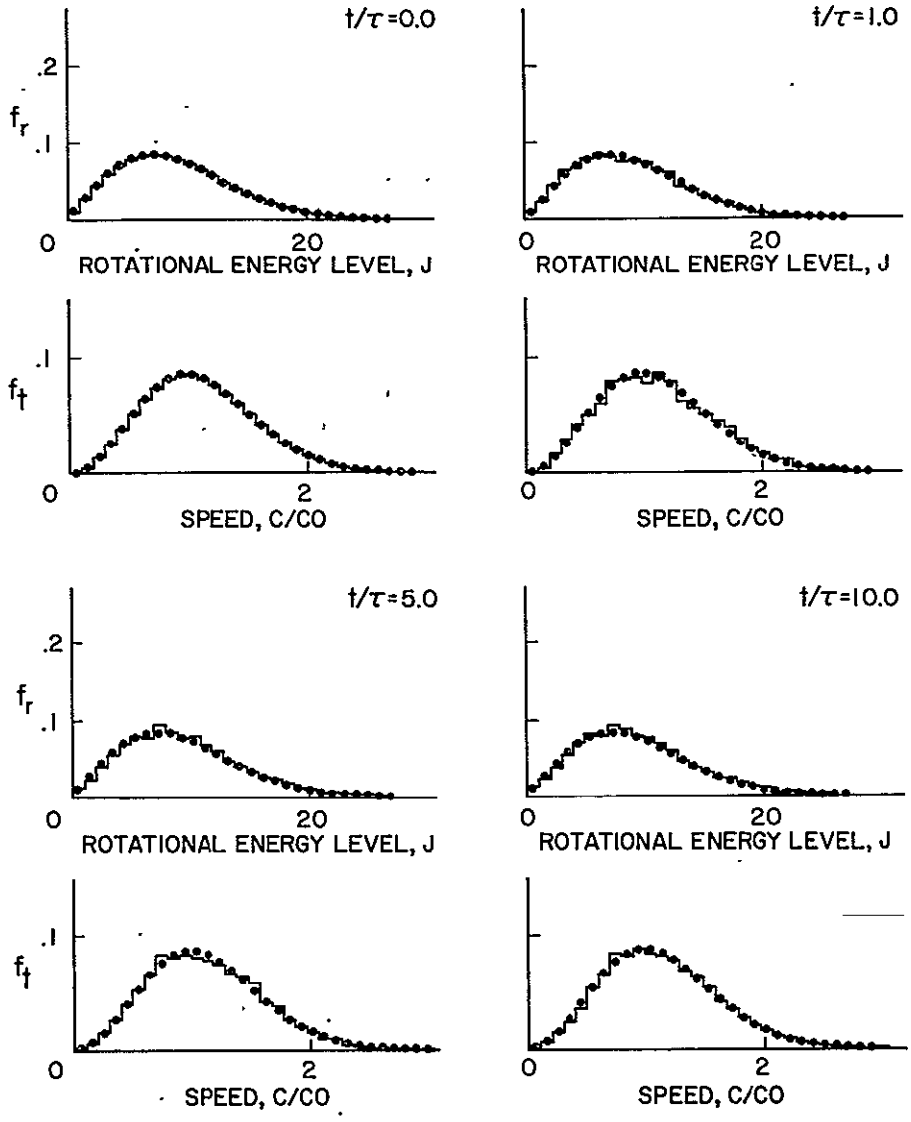

(b) Time average of Monte Carlo results.

Figure 1.- Continued.

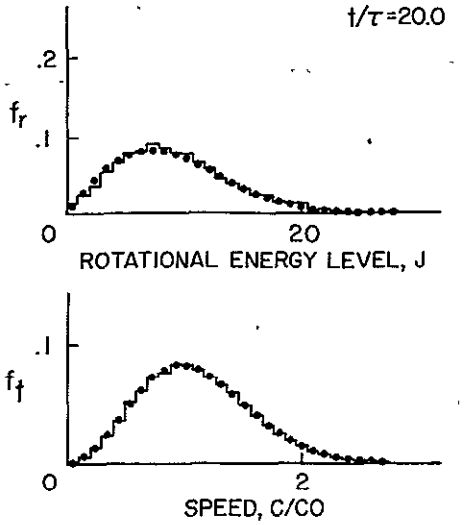

(b) Time average of Monte Carlo results - Concluded.

Figure 1.- Concluded.

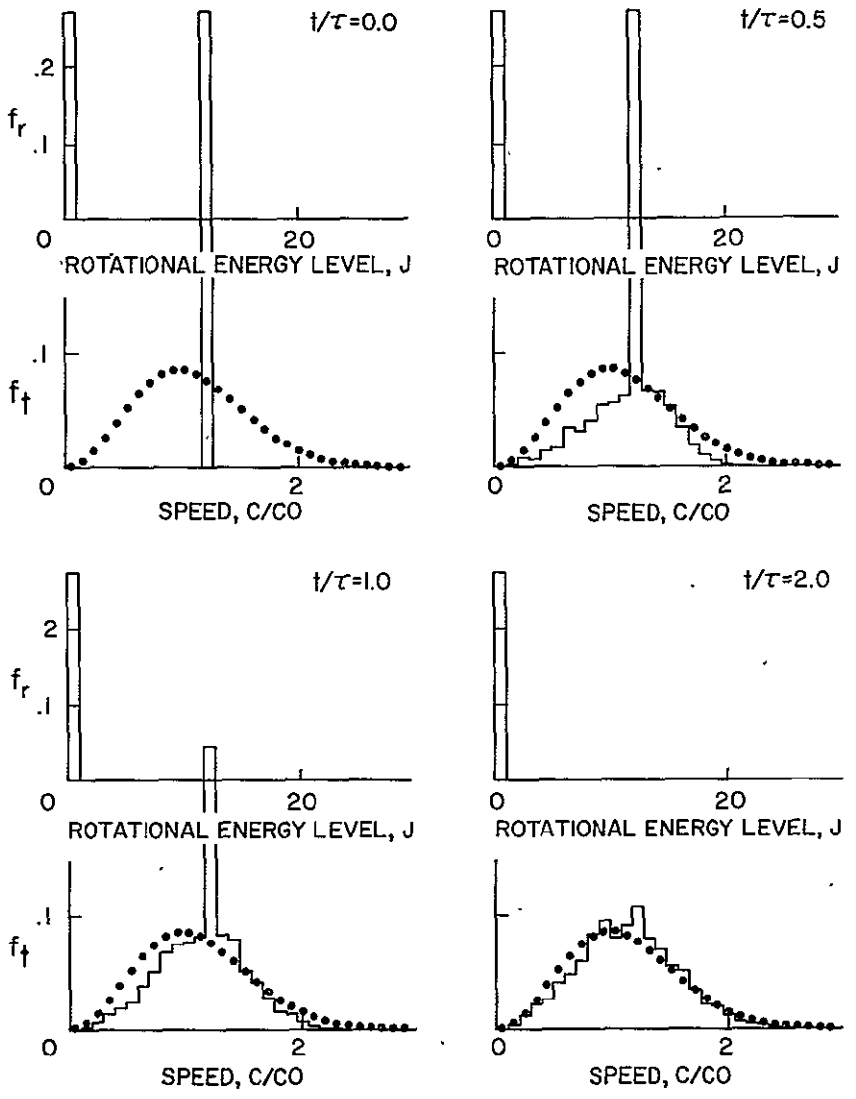

(a) Delta function initial velocity distribution: $f_t(0,x) = 1$ at $x = \sqrt{3/2}$.

Figure 2.- Monatomic gas simulation (rotational effect frozen).

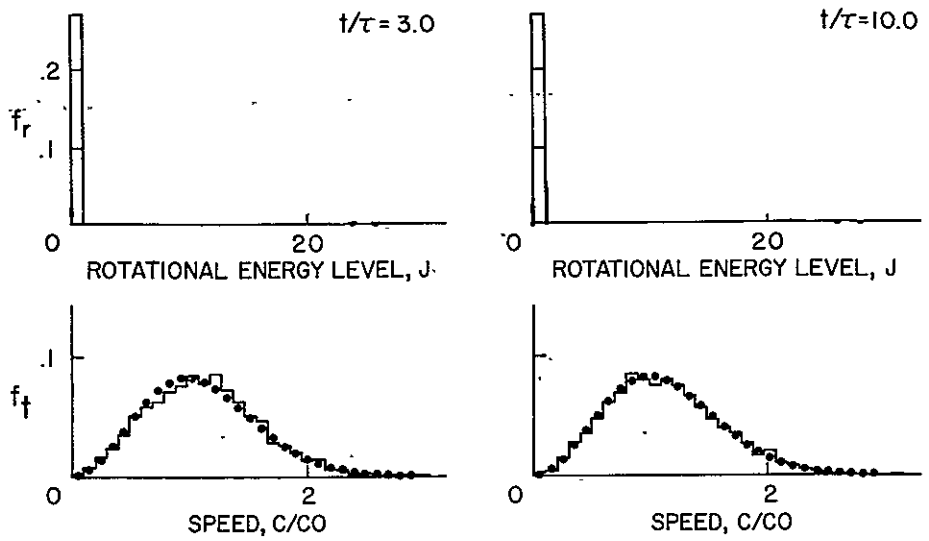

(a) Delta function initial velocity distribution - Concluded.

Figure 2.- Continued.

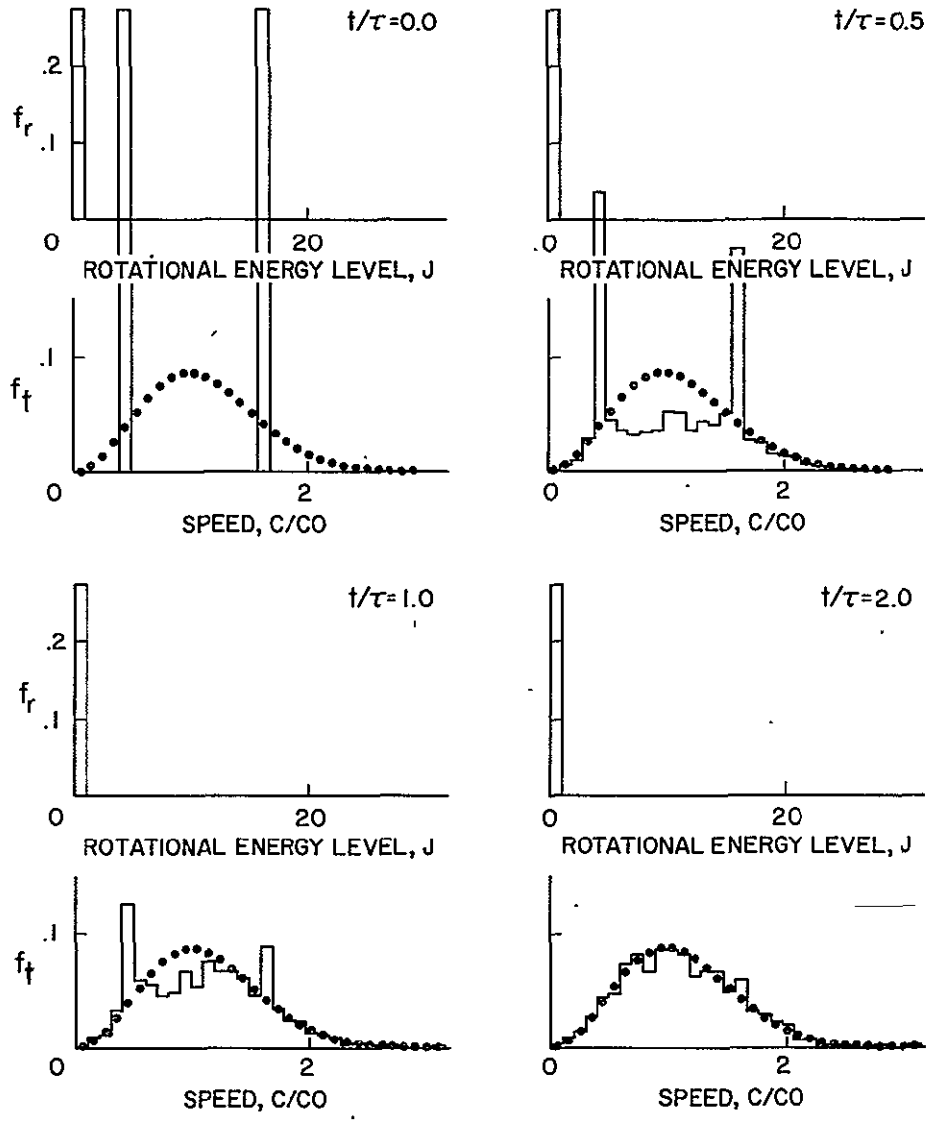

(b) Double delta function initial velocity distributions;
$f_t(0,x_1) = 1/2$ at $x_1 = 1/2$
$f_t(0,x_2) = 1/2$ at $x_2 = \sqrt{11}/2$.

Figure 2.- Continued.

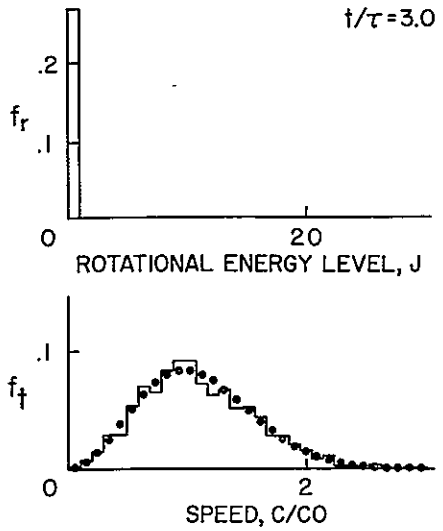

(b) Double delta function initial velocity distributions - Concluded.

Figure 2.- Concluded.

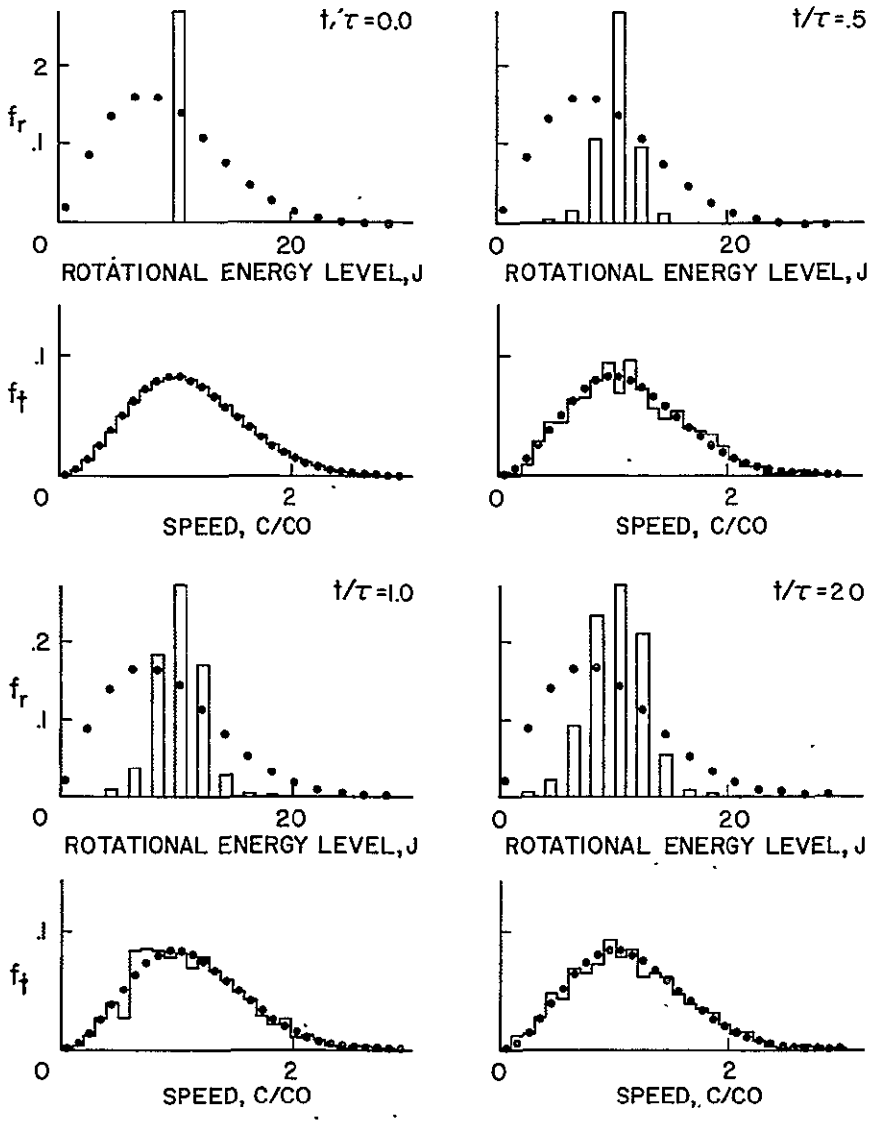

Figure 3.- Maxwellian initial velocity distribution; delta function rotational energy distribution ($f_r(0,x) = 1$ at $j = 10$): Equipartition satisfied.

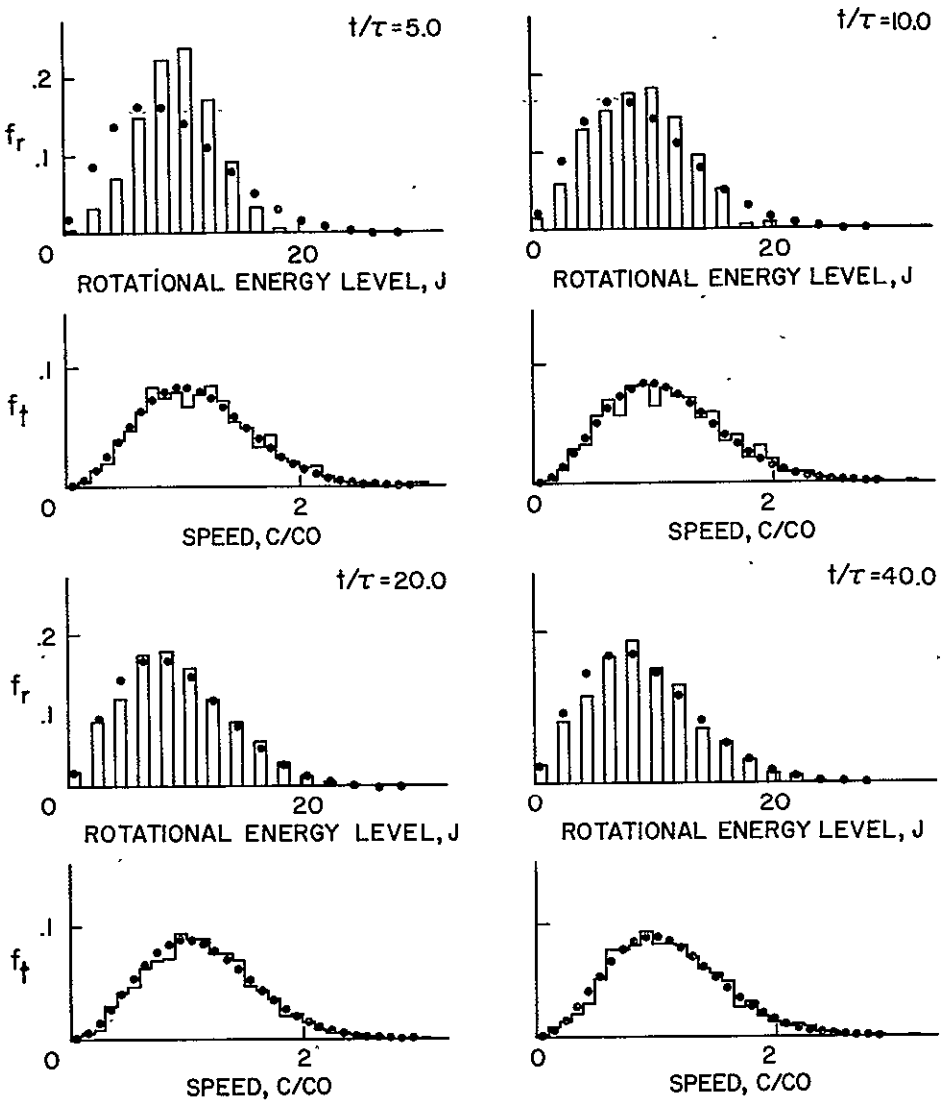

Figure 3.- Continued.

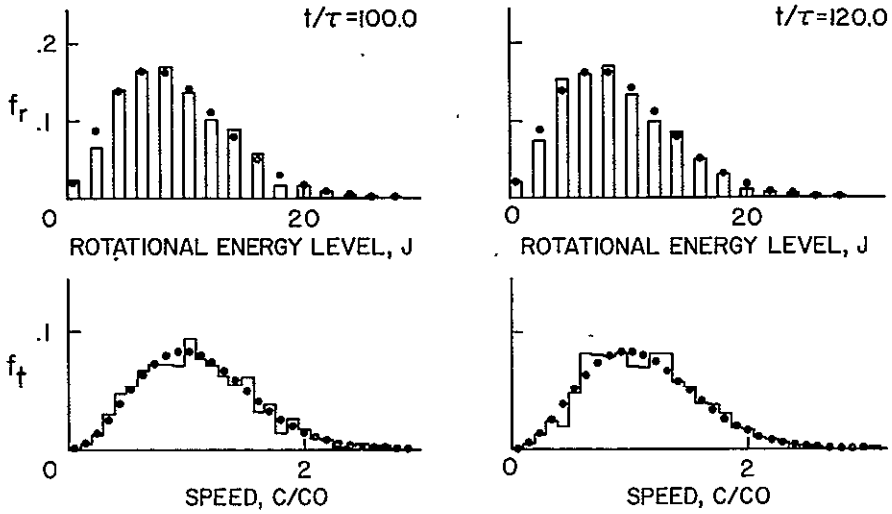

Figure 3.- Concluded.

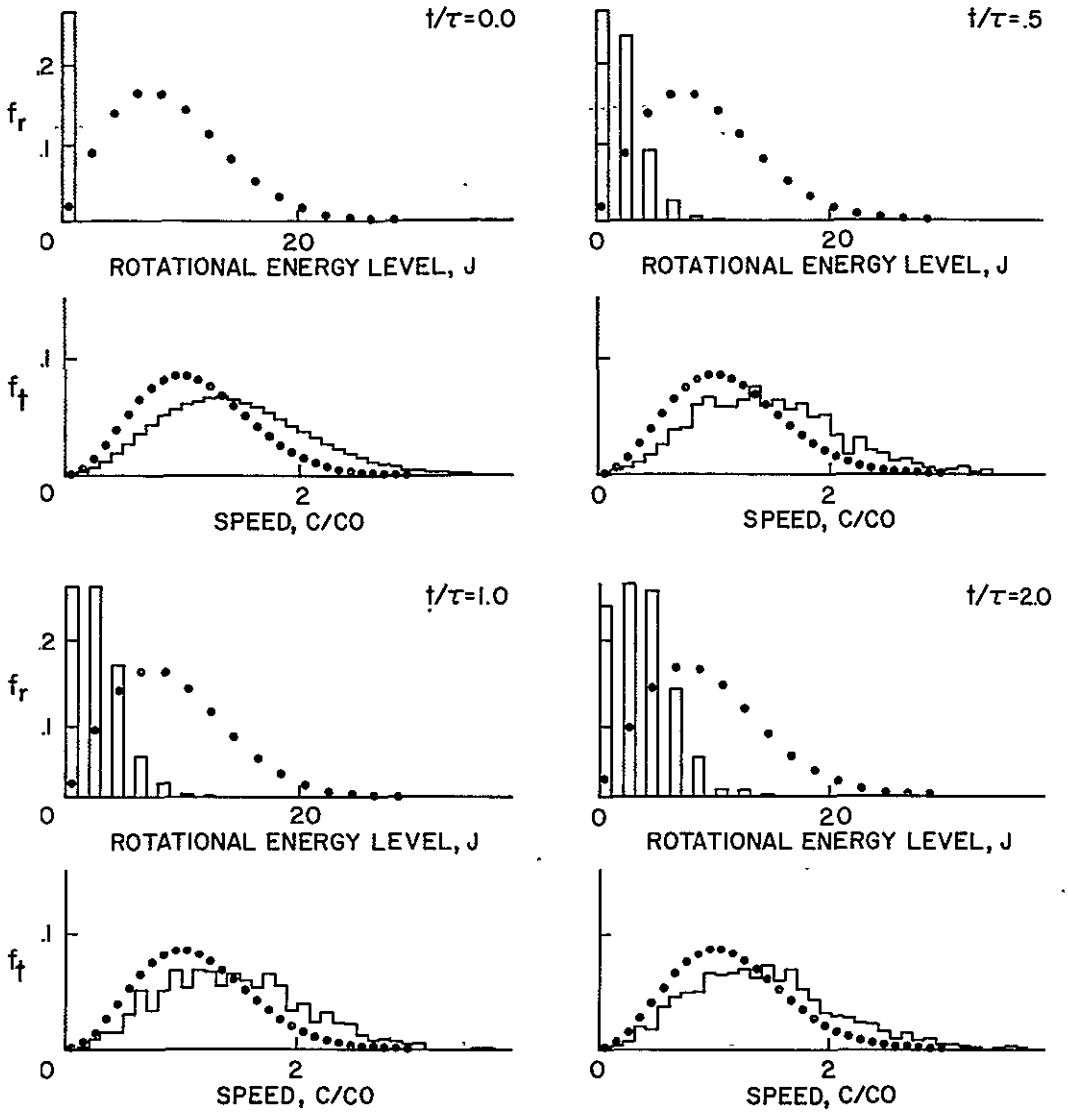

Figure 4.- Maxwellian initial velocity distribution; delta function rotational distribution ($f_r(0,x) = 1$ at $j = 0$): Equipartition not satisfied.

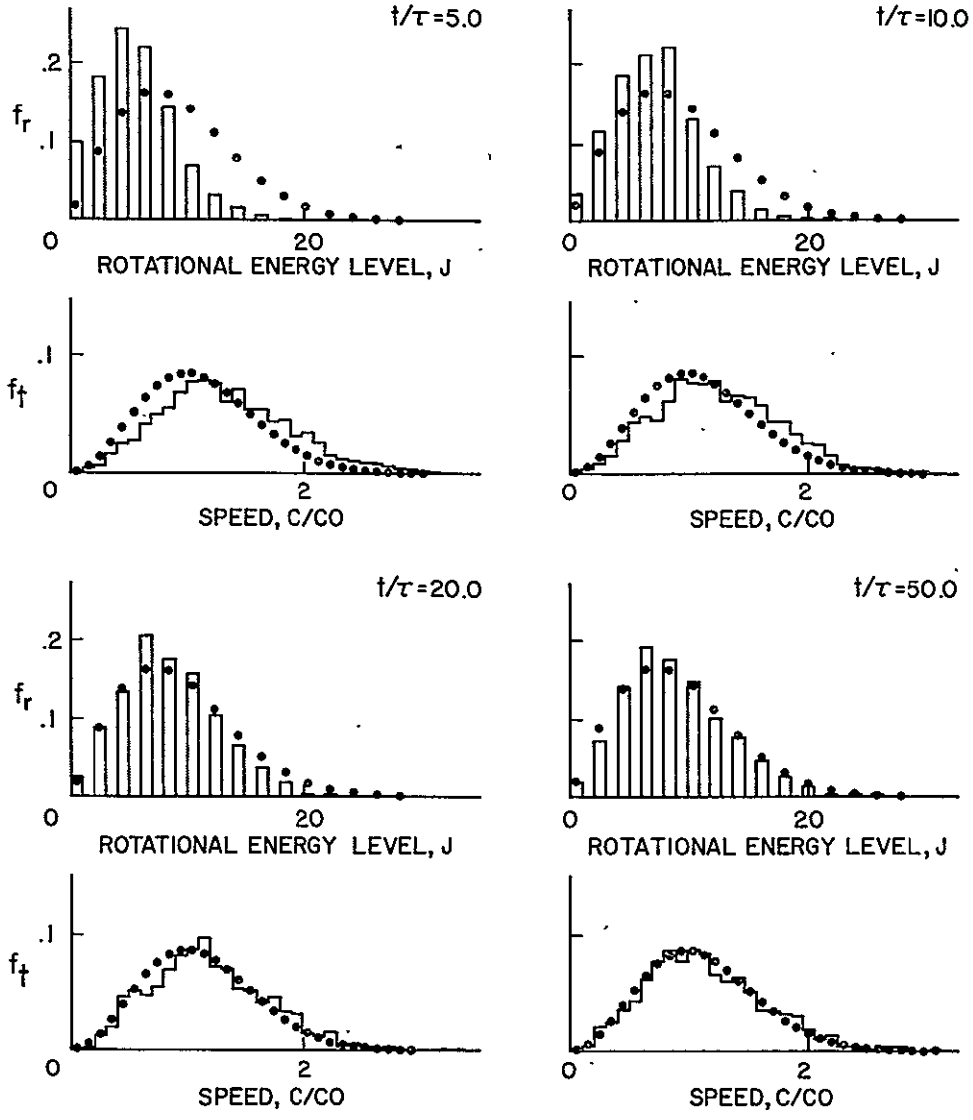

Figure 4.- Continued.

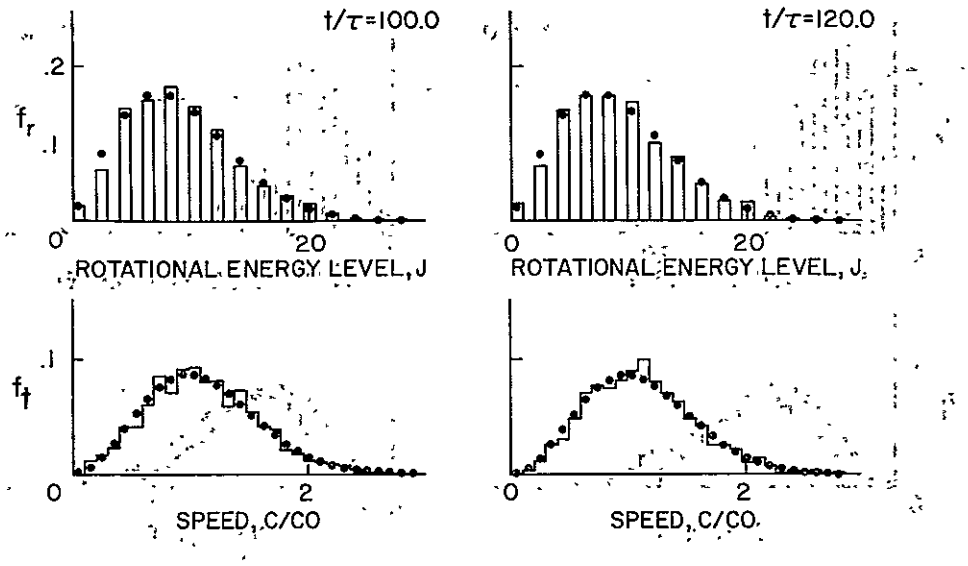

Figure 4.- Concluded.

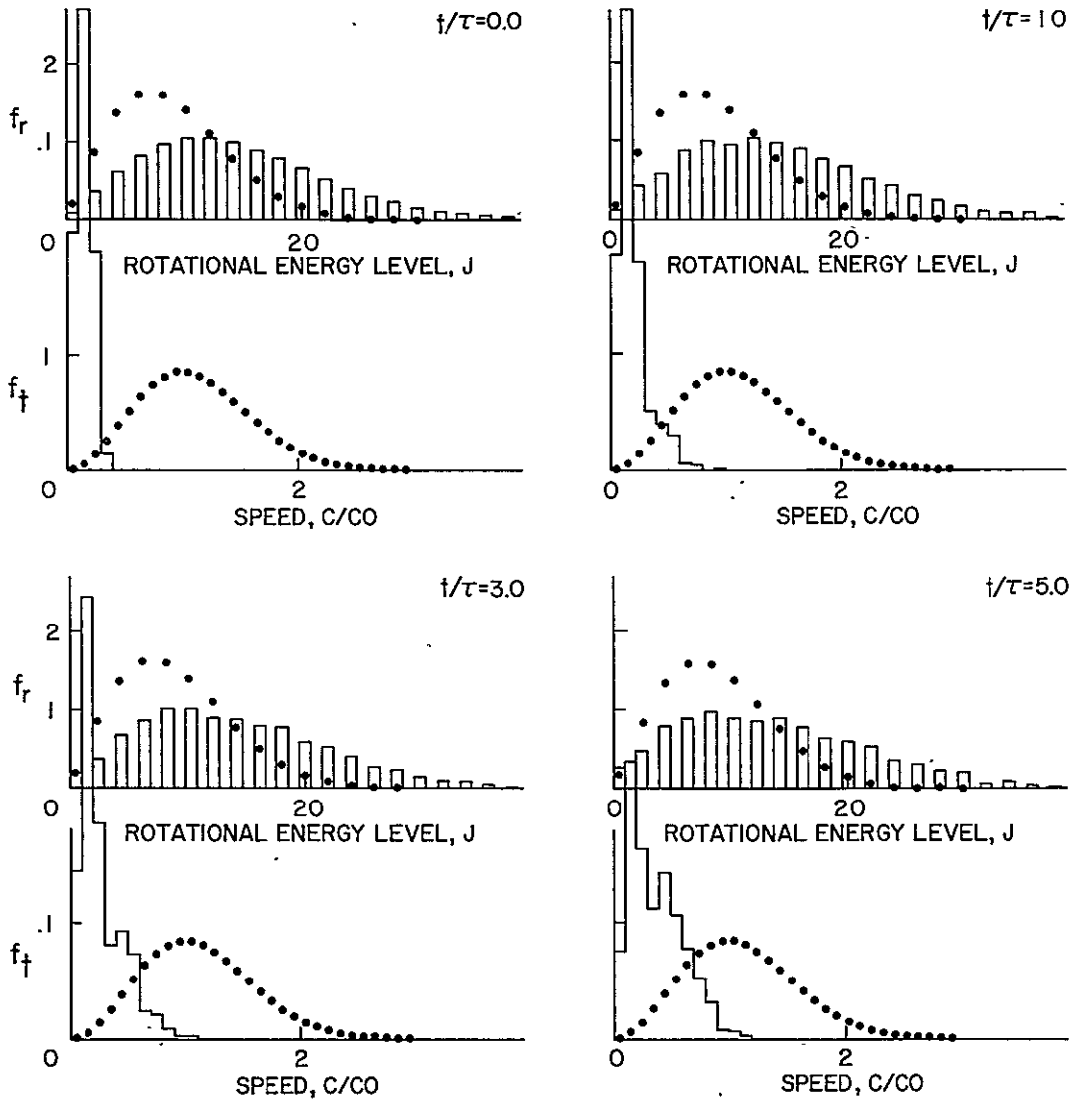

(a) Comparison with equilibrium distributions.

Figure 5.- Maxwellian initial velocity distribution; Boltzmann rotational energy distribution (T_t = 6 K, T_r = 793 K): Equipartition not satisfied.

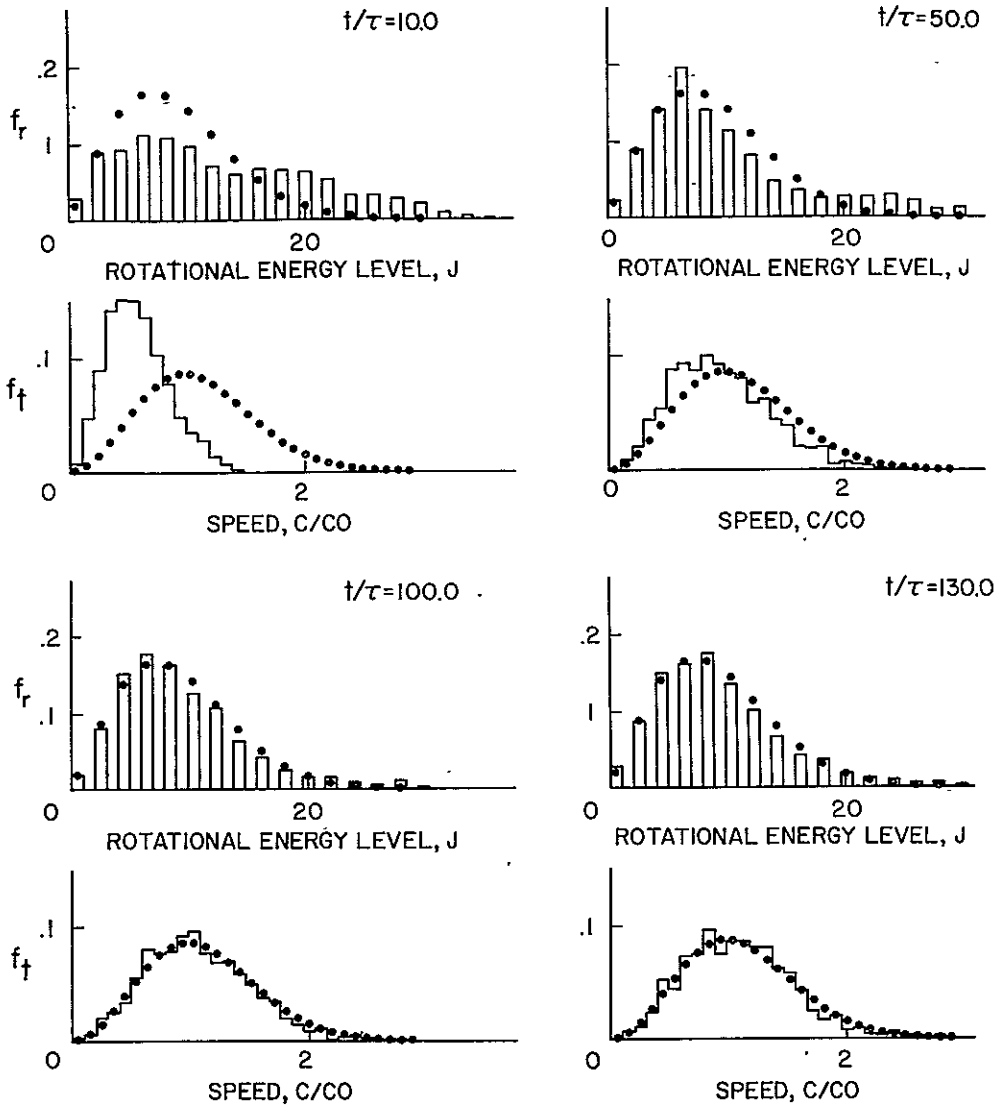

(a) Comparison with equilibrium distributions - Concluded.

Figure 5.- Continued.

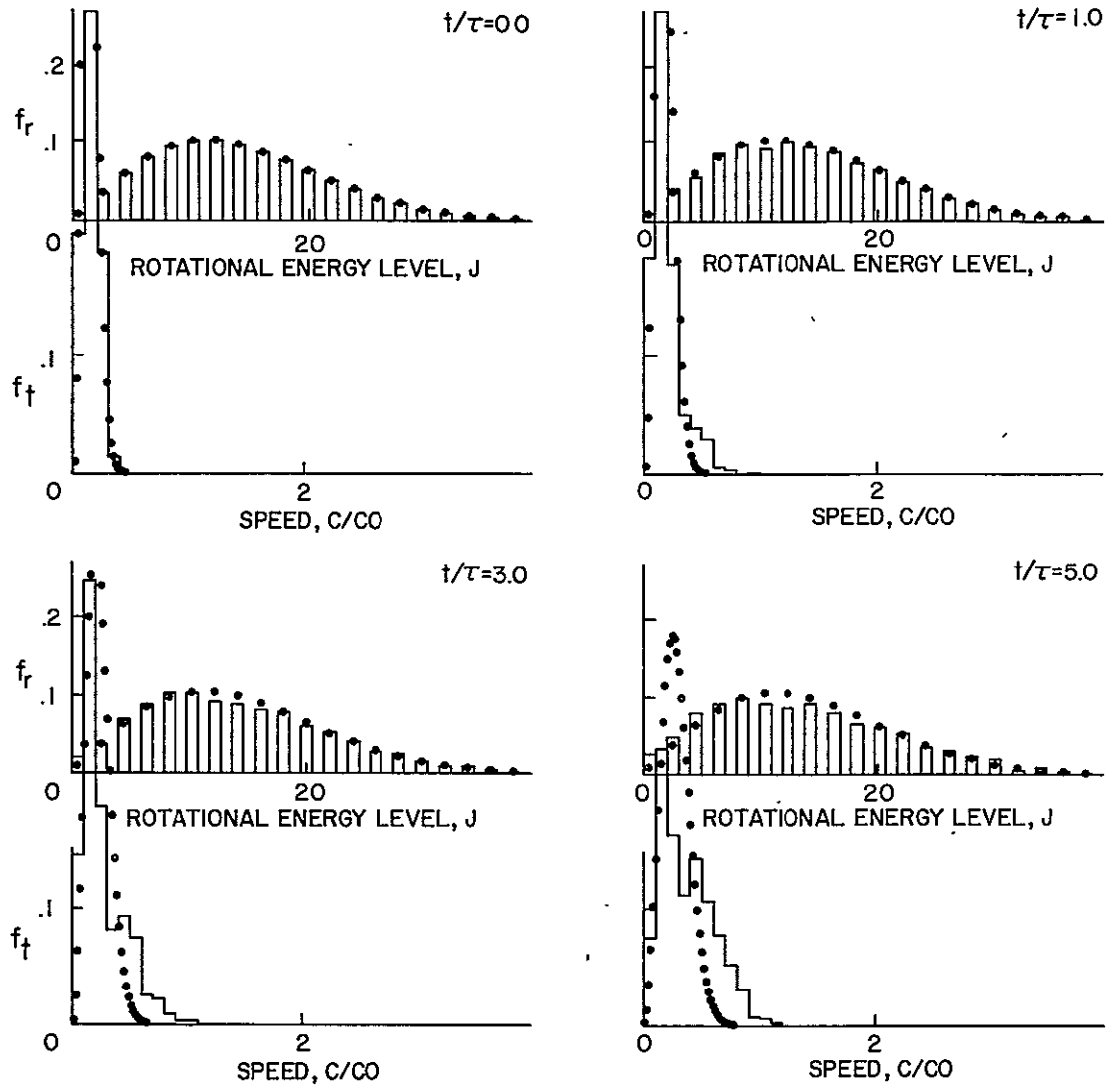

(b) Comparison with local Maxwell-Boltzmann distributions.

Figure 5.- Continued.

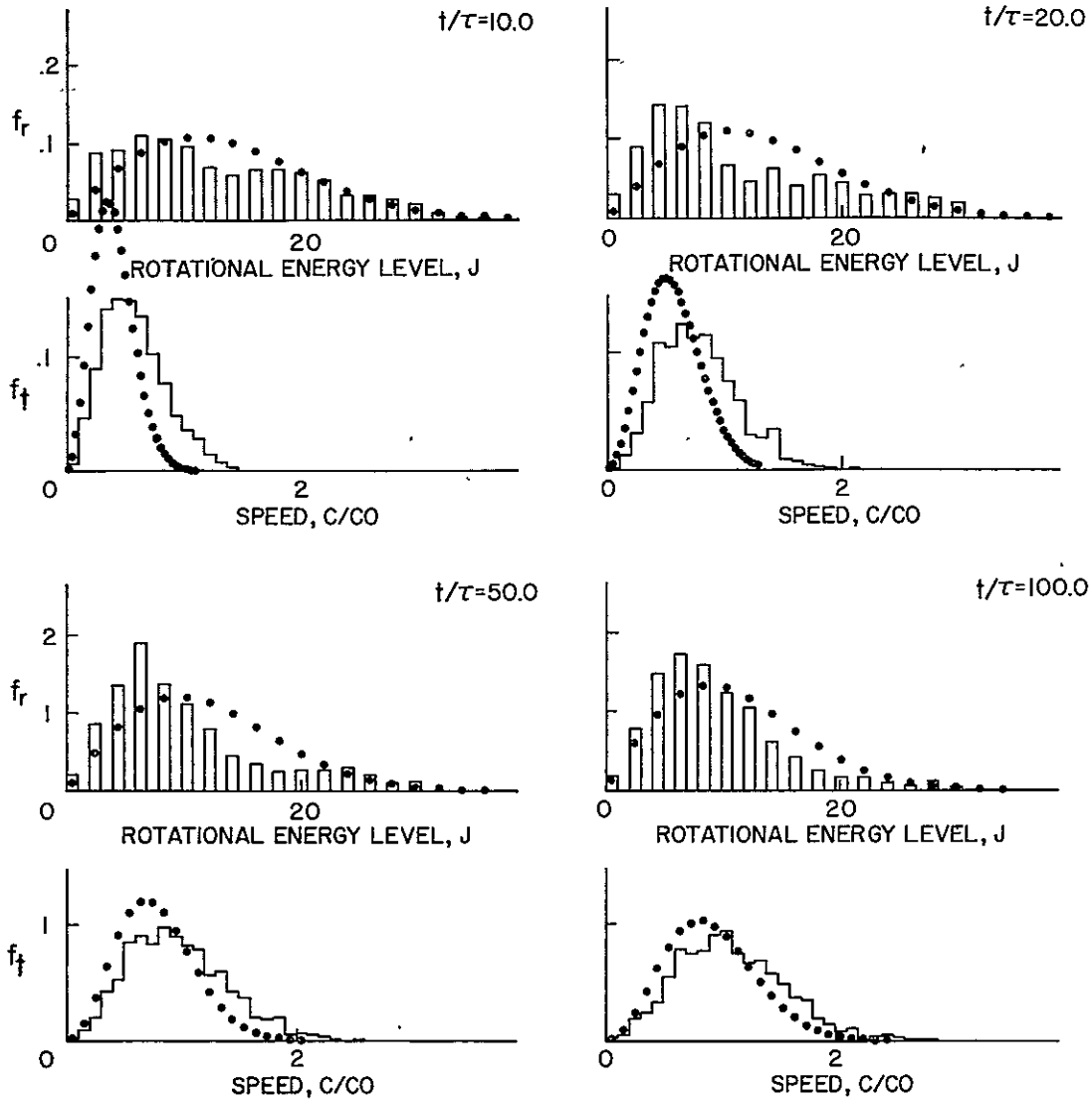

(b) Comparison with local Maxwell-Boltzmann distributions - Continued.

Figure 5.- Continued.

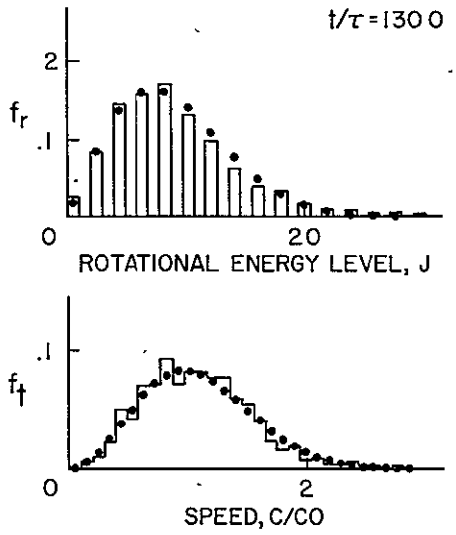

(b) Comparison with local Maxwell-Boltzmann distributions - Concluded.

Figure 5.- Concluded.

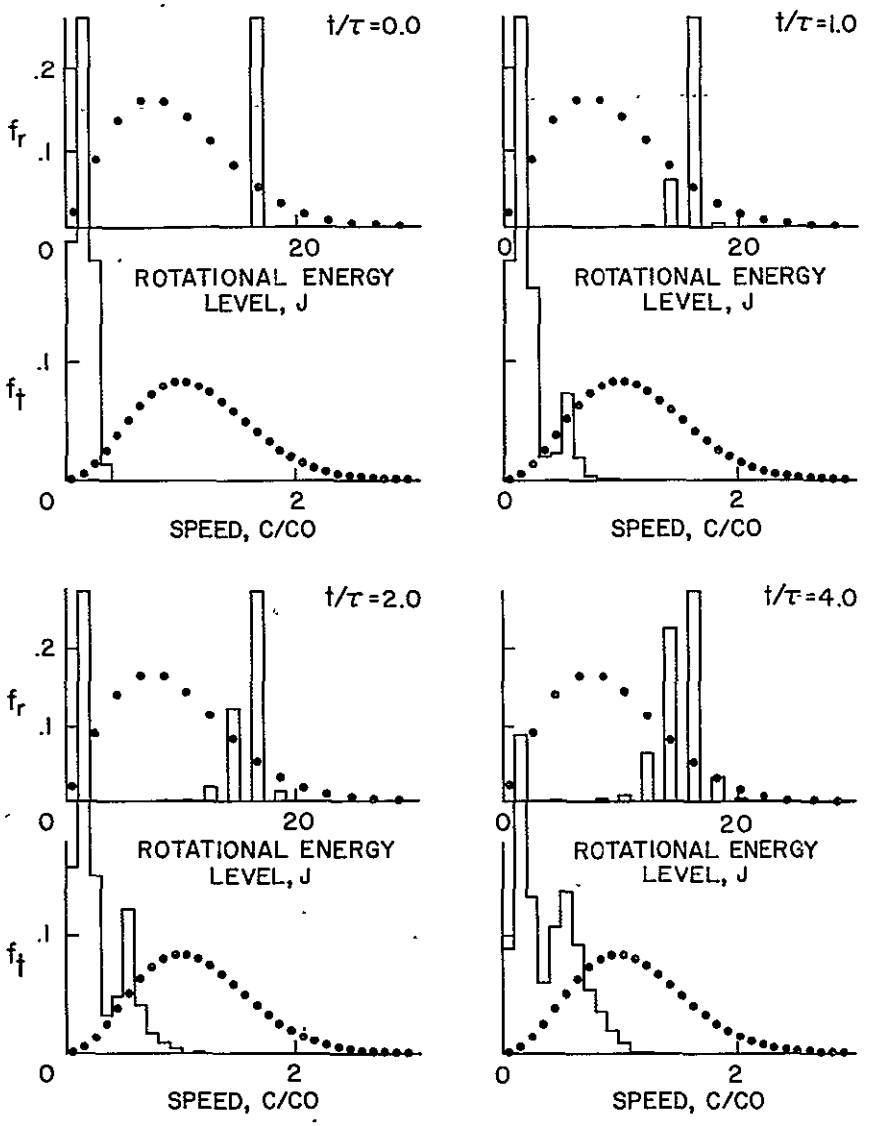

(a) Comparison with equilibrium distributions.

Figure 6.- Maxwellian initial velocity distribution; delta function rotational distribution ($f_r(0,x) = 1$ at $j = 16$); Equipartition not satisfied.

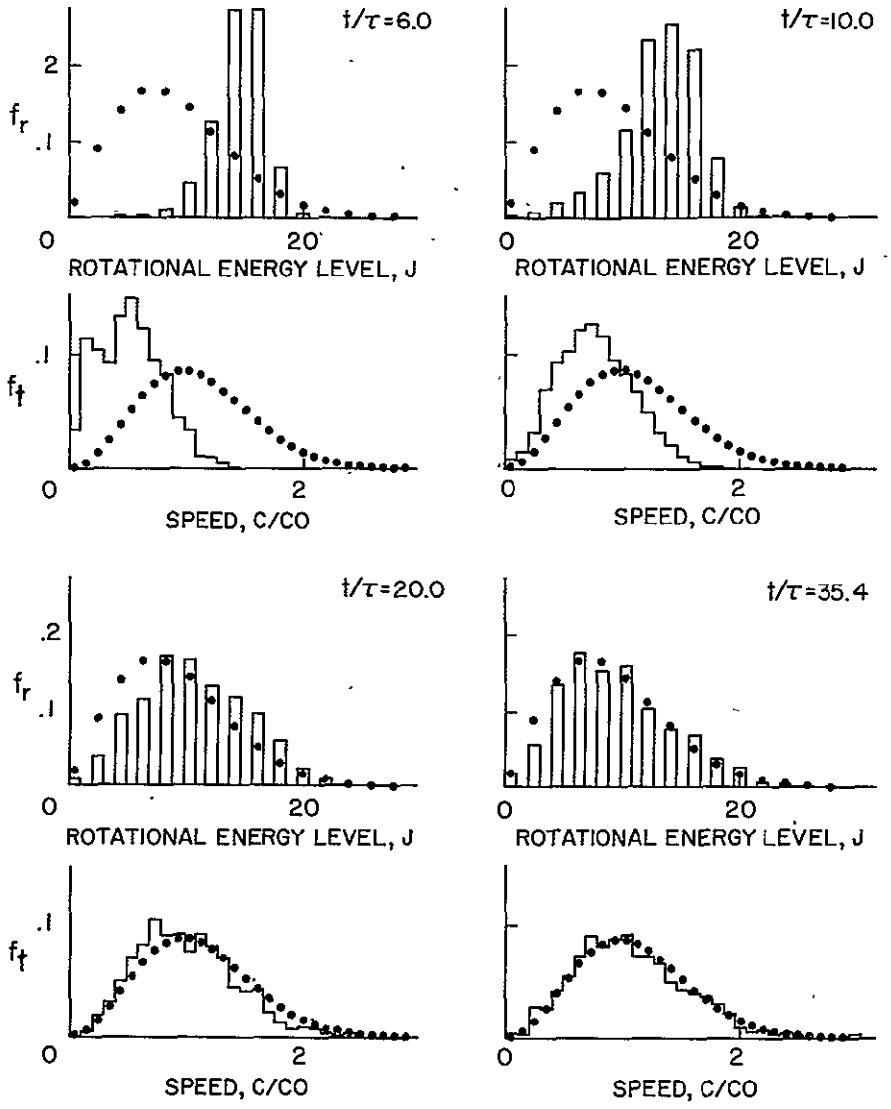

(a) Comparison with equilibrium distributions - Concluded.

Figure 6.- Continued.

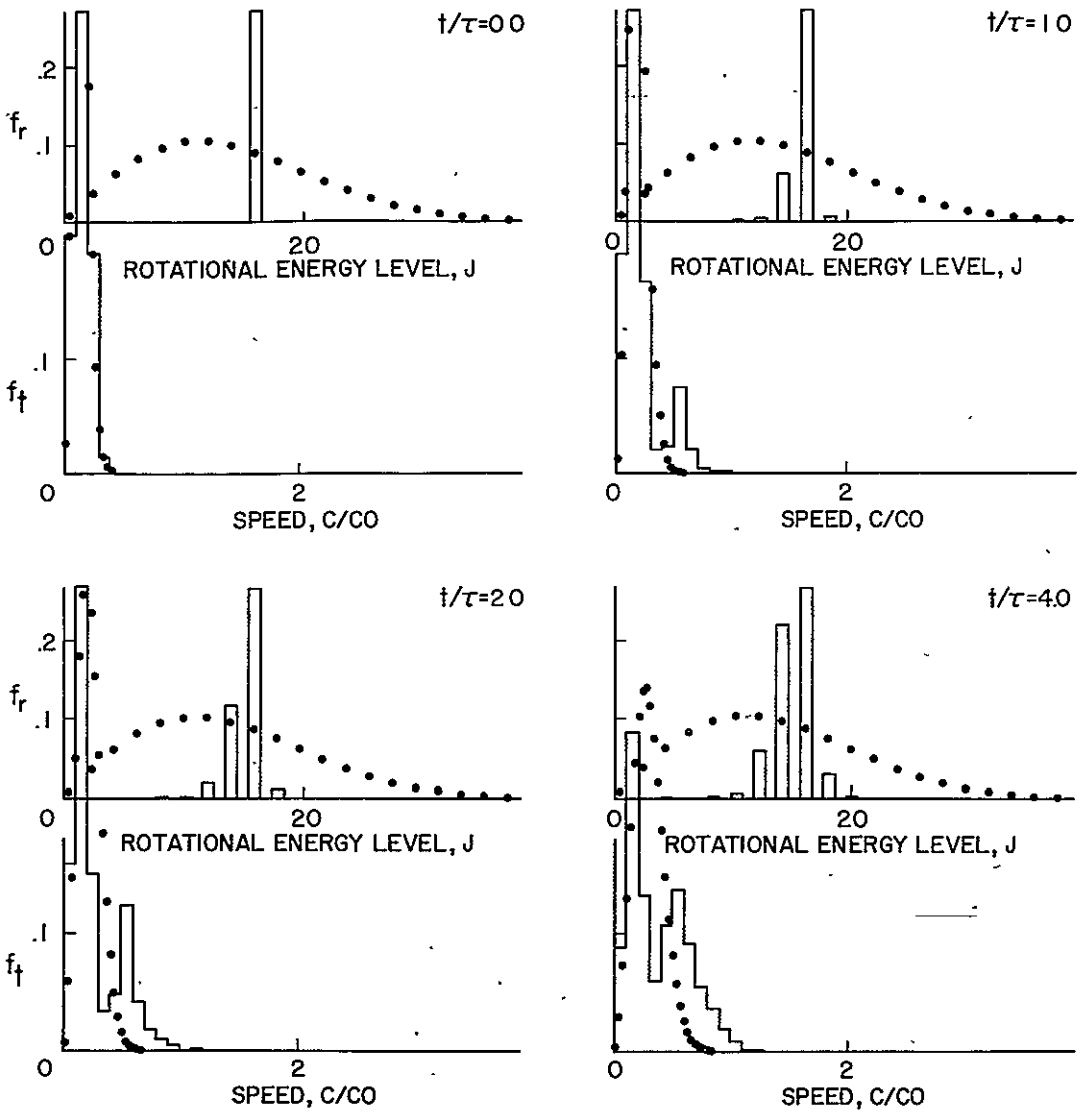

(b) Comparison with local Maxwell-Boltzmann distributions.

Figure 6.- Continued.

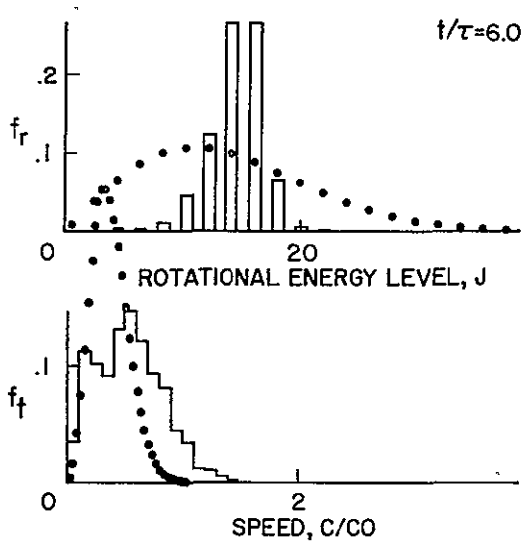

(b) Comparison with local Maxwell-Boltzmann distributions - Concluded.

Figure 6.- Concluded.

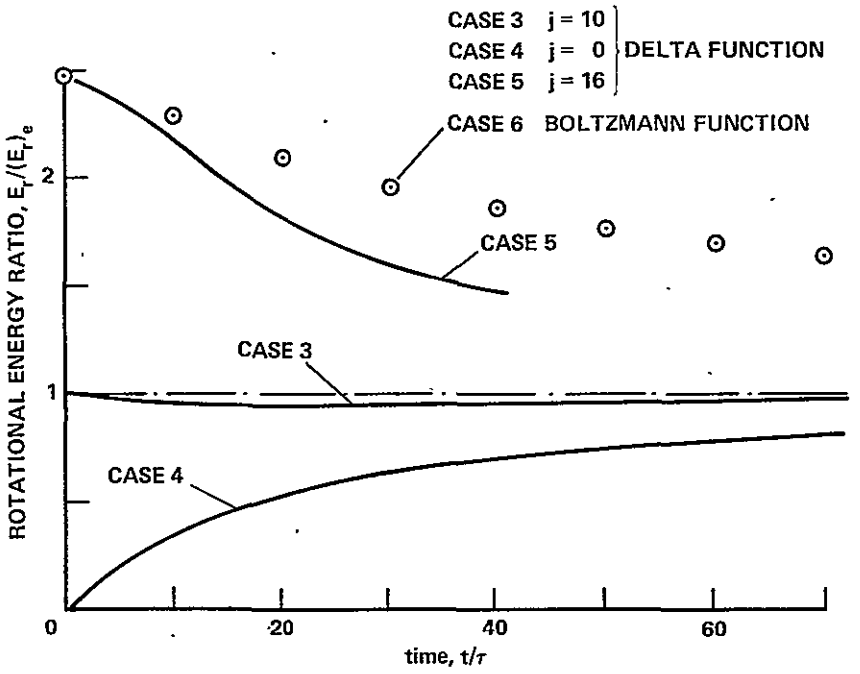

Figure 7.- Relaxation behavior of average rotational energy for a variety of initial distributions.

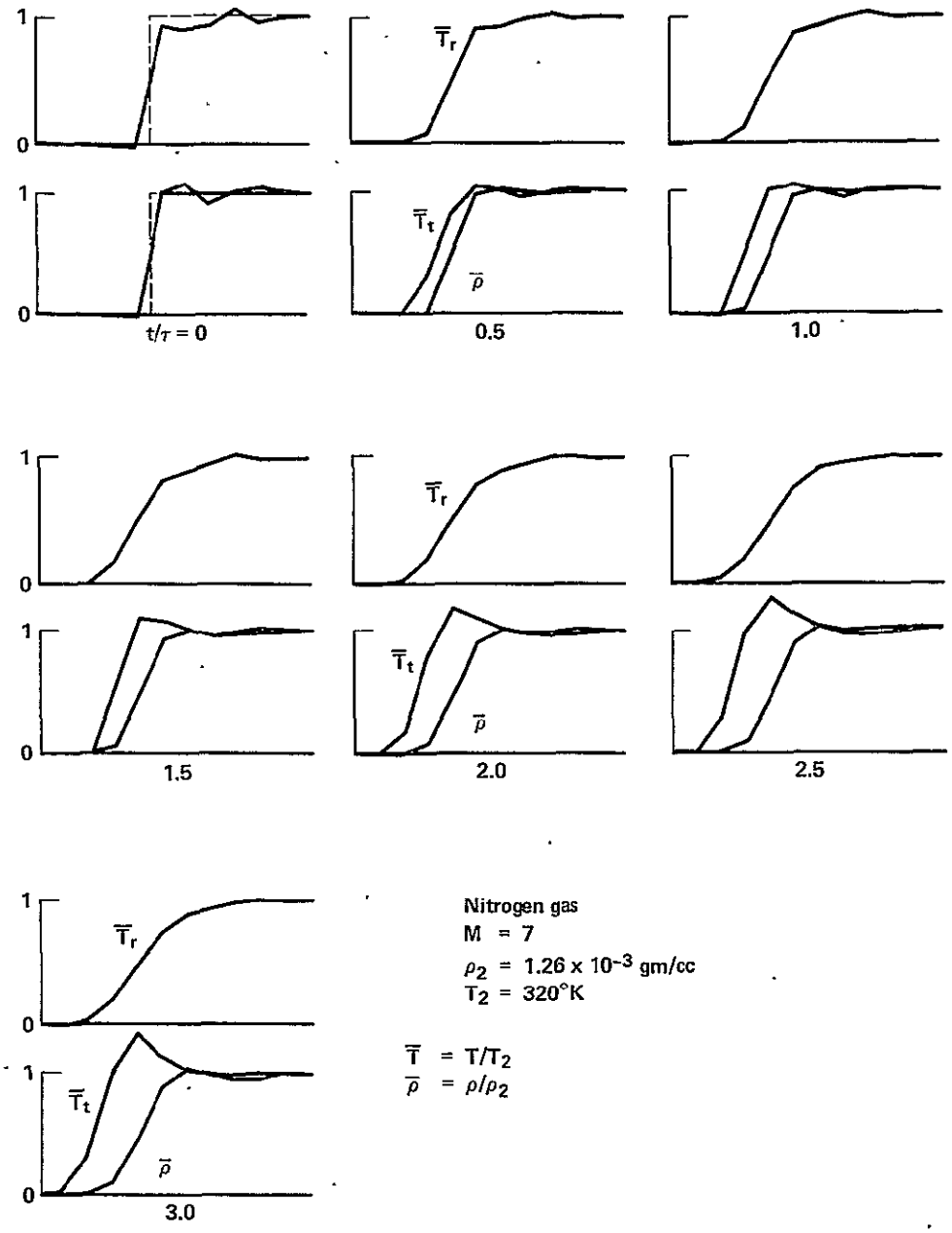

Figure 8.- Preliminary study of shock wave structure.

1. Report No.	2. Government Accession No.	3. Recipient's Catalog No.
NASA TM-78481		

4. Title and Subtitle	5. Report Date
MONTE CARLO SOLUTION OF BOLTZMANN EQUATION FOR A SIMPLE MODEL OF HIGHLY NONEQUILIBRIUM DIATOMIC GASES Translational Rotational Energy Relaxation	6. Performing Organization Code

7. Author(s)	8. Performing Organization Report No.
Kenneth K. Yoshikawa	A-7405
	10. Work Unit No. 505-06-11-01

9. Performing Organization Name and Address	11. Contract or Grant No.
NASA Ames Research Center Moffett Field, California, 94035 and Institute of Space and Aeronautical Science University of Tokyo, Tokyo, Japan (153)	

12. Sponsoring Agency Name and Address	13. Type of Report and Period Covered
National Aeronautics and Space Administration Washington, D.C. 20544	Technical Memorandum
	14. Sponsoring Agency Code

15. Supplementary Notes

16 Abstract

The direct simulation Monte Carlo method is applied to solve the Boltzmann equation for collisions between internally excited diatomic gases in highly non-equilibrium states. The semiclassical transition probability is incorporated in the simulation for energy exchange between rotational and translational energy.

The results provide details on the fundamental mechanisms of gas kinetics where analytical methods are impractical. The validity of the local Maxwellian assumption and relaxation time, rotational-translational energy transition, and a velocity analysis of the inelastic collision are discussed in detail.

17. Key Words (Suggested by Author(s))	18. Distribution Statement
Rarefied gas dynamics Kinetic theory Nonequilibrium thermogasdynamics Mathematical simulation	Unlimited STAR Category - 77

19. Security Classif. (of this report)	20. Security Classif. (of this page)	21. No. of Pages	22. Price*
Unclassified	Unclassified	78	$5.00

*For sale by the National Technical Information Service, Springfield, Virginia 22161